

DEVELOPMENT OF A STRUCTURAL ENGINEERING ORIENTED FINITE
ELEMENT SOFTWARE FEHEAT FOR NONLINEAR HEAT TRANSFER
ANALYSIS

by

İsmail Baş

B.S., Civil Engineering, Bogazici University, 2016

Submitted to the Institute for Graduate Studies in
Science and Engineering in partial fulfillment of
the requirements for the degree of
Master of Science

Graduate Program in Civil Engineering
Boğaziçi University

2020

ACKNOWLEDGEMENTS

I would like to express my sincere gratitude to my advisor Assoc. Prof. Serdar Selamet who guided me in this research. His patience and trust helped me a lot during the difficult times.

I also would like to thank my family for their continuous support throughout the process.

ABSTRACT

DEVELOPMENT OF A STRUCTURAL ENGINEERING ORIENTED FINITE ELEMENT SOFTWARE FEHEAT FOR NONLINEAR HEAT TRANSFER ANALYSIS

An existing structural engineering oriented finite element software, FEHEAT, that can solve two-dimensional heat transfer problems with nonlinear boundary conditions was further developed in this study. The software gained the ability to handle temperature dependent material properties. The tangent stiffness matrix was modified such that it can now consider nonlinear material properties and the heat exchange between surfaces. With this modification, the efficiency of Newton-Raphson nonlinear solution algorithm was significantly increased. Verifications for common scenarios were made with comparing FEHEAT results with commercial finite element software ABAQUS that is a well-known and well-proven software. All results showed that FEHEAT can handle any of these problems with great accuracy. A graphical user interface (GUI) was designed to create inputs using a user-friendly interface for the main code and provide post-processing tools for analysis. Using GUI, one can either model a problem by specifying properties one-by-one or model multiple problems using the interface for parametric modelling. The letter provides a powerful tool for parametric studies. Overall design of software was aimed at providing structural engineers a powerful tool that gives the ability to solve advanced heat transfer problems and both speedup and simplify the modelling phase.

ÖZET

DOĞRUSAL OLMAYAN ISI TRANSFERİ HESABI İÇİN YAPI MÜHENDİSLİĞİ MERKEZLİ SONLU ELEMAN ANALİZİ PROGRAMI FEHEAT'İN GELİŞTİRİLMESİ

Doğrusal olmayan sınır koşulları altında iki boyutlu ısı transferi analizi yapabilen, yapı mühendisliği merkezli mevcut bir sonlu eleman programı olan FEHEAT bu çalışmayla daha da geliştirildi. Program sıcaklığa bağlı değişen malzeme özelliklerini dikkate alabilme özelliğini kazandı. Tanjant rijitlik matrisi doğrusal olmayan malzeme özelliklerini ve yüzeyler arası ısı transferini dikkate alabilecek şekilde düzenlendi. Bu düzenleme ile doğrusal olmayan problemler için kullanılan Newton-Raphson çözüm algoritmasının verimliliği önemli ölçüde geliştirildi. İki boyutlu ısı transferi problemlerinde sık rastlanan senaryolar için FEHEAT sonuçları, bu alanda sık kullanılan ve yeterliliği daha önceki çalışmalarda birçok kez görülmüş olan sonlu eleman programı ABAQUS ile karşılaştırılmıştır. Tüm sonuçlar FEHEAT'in bu problemlerin hepsini yüksek doğrulukla çözebildiğini göstermektedir. Program ana kodu için girdileri kullanıcı dostu bir arayüz ile sunan ve analiz sonuçlarının değerlendirilmesini sağlayan bir grafiksel kullanıcı arayüzü (GUI) geliştirilmiştir. Bu grafiksel kullanıcı arayüzün kullanılarak bir problem özellikleri tek tek girilerek modellenabilir ya da parametrik modelleme için geliştirilen arayüz kullanılarak tek seferde birden çok model oluşturulabilir. Sunulan ikinci seçenek parametrik çalışmalar için güçlü bir araç sunmaktadır. Programın genel tasarımında modelleme aşamasını hem hızlandırıp hem de basitleştirerek yapı mühendislerine ileri düzey problemleri çözme yeteneği kazandıran güçlü bir araç sunmak amaçlanmıştır.

TABLE OF CONTENTS

ACKNOWLEDGEMENTS	iii
ABSTRACT	iv
ÖZET	v
LIST OF FIGURES	viii
LIST OF TABLES	xii
LIST OF SYMBOLS	xiii
LIST OF ACRONYMS/ABBREVIATIONS	xv
1. INTRODUCTION	1
1.1. Background and Motivation	1
1.2. Objectives of the Study	3
1.3. Overview of the Study	4
1.4. Thesis Outline	5
2. THEORETICAL BACKGROUND	7
2.1. Background on Heat Transfer	7
2.2. Finite Element Formulation	11
2.3. Time Stepping Algorithm	13
2.4. Nonlinear Solution Algorithm	16
2.5. Capabilities and Limitations	19
3. VALIDATION	21
3.1. Validation for Rectangular Concrete	21
3.2. Validation with Commercial Finite Element Software ABAQUS	24
3.2.1. Common Case with Linear Material Properties	26
3.2.2. Common Case with Nonlinear Material Properties	30
3.2.3. Insulation Verification	38
3.2.4. Convection Verification	40
4. GRAPHICAL USER INTERFACE (GUI)	43
4.1. Step-by-Step Illustration of ‘Standard GUI Workflow’	45
4.1.1. ‘Material and Geometry Definition’ Menu	45

4.1.2. 'Insulation Data' Menu	47
4.1.3. 'Surface Boundary Conditions' Menu	48
4.1.4. 'Prescribed Temperatures and Heat Fluxes for Nodes' Menu . .	50
4.1.5. 'Cavity Radiation' Menu	51
4.1.6. 'Analysis and Post-Process' Menu	52
4.1.7. 'Nodal Time History Results' Menu	54
4.1.8. 'Sectional Results' Menu	55
4.1.9. 'Field Results' Menu	56
4.2. 'Batch Analysis' Menu	57
4.3. Parametric Modelling Interface	58
5. CONCLUSION	62
5.1. Summary	62
5.2. Possible Improvements	64
5.3. Areas of Use	65
REFERENCES	66

LIST OF FIGURES

Figure 2.1.	View factor calculation [6].	10
Figure 2.2.	Two-dimensional solution domain for general heat transfer in a solid continuum.	12
Figure 2.3.	Flowchart of the FEHEAT algorithm for linear and nonlinear transient heat transfer problem [5].	19
Figure 3.1.	Sketch of the model for the rectangular column.	22
Figure 3.2.	Comparison of temperature distributions obtained using FEHEAT and ABAQUS with Eurocode 2 data.	24
Figure 3.3.	Common case with I Shape (thin) and linear material properties (solid lines represent ABAQUS results, circle marks represent FEHEAT results).	29
Figure 3.4.	Common case with I Shape (thick) and linear material properties (solid lines represent ABAQUS results, circle marks represent FEHEAT results).	30
Figure 3.5.	Change of thermal conductivity coefficient of steel with temperature.	32
Figure 3.6.	Change of specific heat capacity of steel with temperature.	32
Figure 3.7.	Common case with I Shape (thin) and nonlinear material properties (solid lines represent ABAQUS results, circle marks represent FEHEAT results).	33

Figure 3.8.	Common case with I Shape (thick) and nonlinear material properties (solid lines represent ABAQUS results, circle marks represent FEHEAT results).	34
Figure 3.9.	Common case with box section and nonlinear material properties (solid lines represent ABAQUS results, circle marks represent FEHEAT results).	35
Figure 3.10.	Common case with angle section and nonlinear material properties (solid lines represent ABAQUS results, circle marks represent FEHEAT results).	36
Figure 3.11.	Common case with channel section and nonlinear material properties (solid lines represent ABAQUS results, circle marks represent FEHEAT results).	37
Figure 3.12.	Common case with T-Shape and nonlinear material properties (solid lines represent ABAQUS results, circle marks represent FEHEAT results).	38
Figure 3.13.	Insulated case with I-Shape (thin) (solid lines represent ABAQUS results, circle marks represent FEHEAT results).	40
Figure 3.14.	Convection-only case with I-Shape (thin) (solid lines represent ABAQUS results, circle marks represent FEHEAT results).	42
Figure 4.1.	Illustration of GUI workflow.	43
Figure 4.2.	‘Start Screen’ menu.	44
Figure 4.3.	‘Geometry and Material’ menu.	46

Figure 4.4.	‘Temperature Dependent Material Properties’ menu.	47
Figure 4.5.	‘Insulation Data’ menu.	48
Figure 4.6.	‘Insulation Material’ menu.	49
Figure 4.7.	‘Surface Boundary Conditions’ menu.	50
Figure 4.8.	‘Prescribed Temperatures and Heat Fluxes for Nodes’ menu. . . .	51
Figure 4.9.	‘Cavity Radiation’ menu.	52
Figure 4.10.	‘Analysis and Post-process’ menu.	53
Figure 4.11.	‘Nodal Time History Results’ menu.	54
Figure 4.12.	‘Results for Parts’ menu.	55
Figure 4.13.	‘Field Results’ menu.	56
Figure 4.14.	‘Batch Analysis’ menu.	57
Figure 4.15.	‘Post-Processing Menu for Multiple Models’ menu.	58
Figure 4.16.	‘Parametric Modelling Interface’ menu example form for source from file option.	59
Figure 4.17.	‘Parametric Modelling Interface’ menu example form for source from model option.	60

Figure 4.18. ‘Parametric Modelling Interface’ menu example form for source from none option.	61
---	----

LIST OF TABLES

Table 2.1.	Trapezoidal families for time stepping algorithm.	14
Table 3.1.	A summary of verification studies	25
Table 3.2.	Cross-section properties	26
Table 3.3.	Analysis parameters for linear case.	28
Table 3.4.	Analysis parameters for nonlinear case.	31
Table 3.5.	Analysis parameters for insulated case.	39
Table 3.6.	Analysis parameters for convection-only case.	41

LIST OF SYMBOLS

B	Shape function gradient
c	Specific heat
e	Element number
F	Global force vector
F_o	Initial force vector
F_h	Force vector due to convection
F_{ij}	View factor from element i to j
F_{mn}	View factor from subelement m to n
F_q	Force vector due to heat flux on surface
F_T	Force vector due to prescribed temperature
$F_{\sigma,rad}$	Force vector due to radiation
$F_{\sigma,surf}$	Force vector due to cavity radiation
h	Convection heat transfer coefficient
J	Global Jacobian matrix (tangent stiffness matrix)
J_K	Conduction terms in Jacobian matrix (linear conductivity)
$J_{K,NL}$	Conduction terms in Jacobian matrix (nonlinear conductivity)
J_M	Mass terms in Jacobian matrix (linear volumetric heat capacity)
$J_{M,NL}$	Mass terms in Jacobian matrix (nonlinear volumetric heat capacity)
J_{rad}	Radiation (due to fire) terms in Jacobian matrix
J_{surf}	Cavity radiation terms in Jacobian matrix
k	The thermal conductivity coefficient
K	Global heat convection matrix including convection
K_c	Global heat conduction matrix
K_h	Global heat convection matrix
m	Number of subelements in element i

M	Mass matrix
n	Number of subelements in element j or current time step
N	Shape function
q_n	Heat flux per unit area in surface normal direction
q_x	The heat flux in x-direction
R	Unbalanced heat vector
$S_{0,m-n}$	Distance between subelements
T	Temperature
T_0	Initial temperature
T_{fire}	Fire temperature
\tilde{T}_{n+1}	Predicted temperature field for the next step at the current iteration
T_s	Surface temperature
TOL	Newton-Raphson algorithm tolerance
v	Velocity
v	Initial velocity
Γ	Surface
Δt	Time increment
Δt_{cr}	Critical time increment
ε_r	Emissivity coefficient for surfaces exposed to fire
ε_{surf}	Emissivity coefficient for surfaces exposed to fire
θ	angle between the surface normal and the distance vector
ρ	Density of the material
σ	Stefan-Boltzmann constant
Ω_e	Surface
$[\]$	Matrix associated with the enclosed quantity
$\{ \}$	Column vector associated with the enclosed quantity
$[\]$	Row vector associated with the enclosed quantity

LIST OF ACRONYMS/ABBREVIATIONS

<i>1D</i>	One-Dimensional
<i>2D</i>	Two-Dimensional
<i>3D</i>	Three-Dimensional
<i>FEM</i>	Finite Element Method
<i>GUI</i>	Graphical User Interface

1. INTRODUCTION

1.1. Background and Motivation

Fire is a great treat to (especially steel) structures. Between 2007–2011, 15,400 structural fires have been reported in the U.S. alone claiming an annual average of 46 civilian lives, 530 injuries and \$219 million in direct property damage [1]. The evaluation of the performance of structures under fire relies heavily on how accurately the temperature distribution on structural members are determined. For some cases, some simplified approaches might be developed but in general, it requires a careful study.

A common practice is to use a prescriptive and code-based approach for fire evaluation. This approach helps make design considerations practically and can still be considered as the main approach in the industry currently. Another aspect of this approach is that it generally does not require the decision-maker to be an engineer since most considerations are based-on tables and figures that are obtained by making many assumptions.

However, with increasing computation power and the developed analysis algorithms proven to be accurate, prescriptive approach is increasingly being replaced by the performance-based approach. In this approach, the design of the fire protection strategy and structural detailing of a building is based on evaluating the structure's behaviour under more realistic and project-based fire scenarios. Performance-based approach requires the decision-maker to be from an engineering background and able to understand the theoretical background of the problem. With this new approach, the structural fire engineers gain the ability to play more role in fire design and more engineered solutions can be obtained. Thus, the accurate determination of temperature distribution on a cross-section under a fire scenario has gained more importance in structural fire engineering practice.

For fire performance evaluation, numerical methods are proven to be more advantageous in various ways than experimental studies. Experimental tests on fire are generally time-consuming and very expensive. Numerical methods provide much faster solutions than experimental tests, and they cost much less. One of the most advantageous sides of numerical methods is that they can provide a more flexible environment for parametric studies.

There are analytical solutions to heat transfer problems, but they are only applicable to 1-D problems and very simple 2-D problems. With increased complexity, analytical solutions become insufficient and use of numerical methods become a must in calculations. Finite difference methods are also used for simple problems and have limited capabilities. Finite element methods (FEM) have become the most practical and reliable solution in most of the problems faced in industry and academy.

There are general-purpose finite element software like ABAQUS [2], ANSYS, ADINA, HEATING and Comsol that provide the ability to conduct advanced 2D and 3D heat transfer analysis. For example, ABAQUS provide options on temperature dependent material properties, surface heat exchange (cavity radiation) and nonlinear boundary conditions as necessary for a structural fire engineering problem. It also can handle any 2D or 3D geometry with tools on mesh generation.

Common practice in structural fire engineering (apart from more simplified approaches) is to conduct a 2D heat transfer analysis on the cross-section with fire boundary conditions. But these general-purpose software are not designed only for 2D heat transfer analysis and with all the other features they provide they are generally an expensive option for structural fire engineering practice. Additionally, the users generally must define properties like cross-sections, materials, fire curves etc. and must arrange most of the analysis options by themselves. That requires the user to know both the theoretical background of the analysis and the software interface very well to conduct a simple 2D heat transfer analysis. Thus, there is a need for problem-specific software for 2D heat transfer analysis to solve common problems faced in industry.

TASEFplus [3] and SAFIR [4] (which was an inspiration for FEHEAT) are examples of programs that have been developed specifically for heat transfer problems. They both can handle temperature dependent material properties and boundary conditions. Both these codes provide the capability for modelling heat transfer by cavity radiation as well.

1.2. Objectives of the Study

This study is mainly focused on further development of existing finite element software FEHEAT that will provide the ability to conduct advanced 2-D heat transfer analysis to use of structural fire engineers. FEHEAT has had most of the analysis capabilities required in this field in earlier versions. With this study, further development of FEHEAT is aimed with modifications to the nonlinear solution algorithm and a powerful graphical user interface that it lacked in previous versions.

With a simple and user-friendly interface, built-in libraries and other features that are provided by GUI, modelling phase is made both faster and more error-free. Thus, it is aimed to make FEHEAT a practical tool that structural fire engineers use in their daily projects.

Providing batch run capabilities, it is aimed that multiple runs can be coordinated at once in case some heavy models are to be run and/or the number of models to be run is so many such that separate handling of the models become hard.

Parametric modeling interface is created with an aim that this software will be a powerful modelling tool for parametric studies in structural engineering field for heat transfer analysis. This tool also makes FEHEAT suitable for academic studies on parameters effecting temperature distribution based on any scenario.

1.3. Overview of the Study

FEHEAT was first developed by Serdar Selamet [5] by modifying the linear beam matrix analysis program written by Prof. Jean Prevost at Princeton University for the course titled “Introduction to Finite Element Methods (CEE513)” The program evolved to a finite element analysis program that can solve two-dimensional transient heat problems with nonlinear boundary conditions.

First version of the program did not have support for material nonlinearity and surface heat exchange (cavity radiation). Later, the capability of calculating surface heat exchange was added within the study [6]. But the effect of the surface heat exchange on the tangent matrix as described in Section 2.4 was not taken into account in [6].

With this study, additional terms due to the surface heat exchange are now added to the tangent matrix during nonlinear analysis. This was a major step in speeding up the solution algorithm since it decreased the amount of iterations performed in each step (especially late steps where the error increases with elevated temperature). The code used for analysis were improved. The solution algorithm of the code was developed, and the analysis run-time was cut up to 10 times for the trial analyses.

Within the scope of this study, the ability to consider temperature dependent material properties was added to FEHEAT. For this implementation, the tangent stiffness matrix was modified to introduce the effect of nonlinearity in material. Nonlinearities in both the thermal conductivity coefficient and the specific heat capacity of the material are now considered by FEHEAT if desired by the user.

FEHEAT only supported I-Shapes in both of the previous versions mentioned above. Box, angle, channel, T-shape and solid rectangle are now supported in addition to I-shape. Mesh generation tools were developed for each cross-section type. GUI menus were redesigned for new supported cross-section types. FEHEAT now supports

most of the common libraries for all cross-section types. FEHEAT uses only quad element, which is enough to obtain appropriate mesh for all cross-sections currently supported.

A graphical user interface (GUI) was designed such that for most cases, the user does not have to define a new cross-section, material, fire curve and other properties since built-in libraries exist for all properties. Custom properties can also be specified when necessary.

FEHEAT works in MATLAB [7] environment which is a common environment in academic studies and engineering practices. It provides special features for use of engineers and academics apart from being a programming language. Error handling and product development is also made easier with a huge community of engineers. Both the main code and the GUI use MATLAB functions and menus organized together as a finite element software.

1.4. Thesis Outline

This thesis consists of five chapters. Background and motivation for this study followed by the objectives and overview of the study are given in Chapter 1.

Background on heat transfer, finite element formulation, time stepping algorithm, nonlinear solution algorithm and capabilities and limitations are given in Chapter 2.

Validation with temperature distribution data provided in Eurocode 1 [8] for rectangular concrete shapes and validation with commercial finite element software ABAQUS are provided in Chapter 3.

Step-by-step illustration of ‘Standard GUI Workflow’, ‘Batch Analysis’ menu and ‘Parametric Modelling Interface’ are given in Chapter 4.

Finally, summary of the study followed by the possible improvements and areas of use for the software are given in Chapter 5.

2. THEORETICAL BACKGROUND

The developed code can solve transient heat transfer problems with nonlinear boundary conditions (radiation etc.) considering temperature dependent thermal properties of the material. A brief background information on the heat transfer is provided in Section 2.1. Finite element formulation for two-dimensional heat transfer problem considering radiation, convection, surface heat exchange, Dirichlet and Neumann boundary conditions is developed in Section 2.2. Time stepping algorithm used for analysis is explained in Section 2.3. Then, Nonlinear solution algorithm is explained in Section 2.4. Finally, the capabilities and limitations of FEHEAT are given in Section 2.5.

2.1. Background on Heat Transfer

There are three modes of heat transfer: conduction, convection and radiation.

Conduction is the heat transfer within a medium due to a diffusion process. It is governed by the Fourier heat conduction law given in Eq.(2.1) which shows a linear relationship between temperature gradient and the heat flow. The proportionality is denoted by a coefficient called thermal conductivity k .

$$q_x = -k \frac{\partial T}{\partial x} \quad (2.1)$$

Where q_x , T and x denote the heat flux per unit area in x direction, the temperature and the direction on which the heat flux is to be calculated, respectively. Since heat transfer analysis is to be conducted on a solid, conduction is the main mode of heat transfer that every element in the model will experience. Thermal conductivity coefficient k is specific to the material and determined by conducting experiments. It can be dependent on the temperature of the material but in general it changes slowly with temperature.

Convection is the heat transfer through a fluid due to the motion of the fluid. It is governed by Newton's law of cooling given in Eq.(2.2) which states that heat flow is proportional to the temperature difference between the two media with a coefficient called convection heat transfer coefficient h . Convection heat transfer coefficient is also known as film conductance.

$$q_n = h(T_s - T_{fire}) \quad (2.2)$$

Here, q_n is the heat flux per unit area due to convection in surface normal direction, T_s is the surface temperature and T_{fire} is the gas (fire) temperature.

Convection heat transfer coefficient is determined empirically due to the complexity of the interaction between gas and the heated surface. In most of the structural fire engineering practices convection heat transfer coefficient is taken as constant throughout a surface. As the heat flux depends on the surface temperature, it still needs a special handling on surfaces.

Radiation is the electromagnetic energy emitted by a medium due to the temperature of the medium. The radiant energy emitted by the surface due to fire is calculated using the Stefan-Boltzmann law as follows:

$$q_n = \sigma \varepsilon_r (T_s^4 - T_{gas}^4) \quad (2.3)$$

where q_n is the heat flux due to the radiation, σ is known as Stefan-Boltzmann constant, ε_r is the emissivity constant and represents the ratio of the energy emitted by the surface to the total energy absorbed, T_s and T_{fire} are the surface and gas (fire) temperatures in Kelvin.

Emissivity constant must be less than one by definition since the amount of energy emitted cannot be more than the amount of energy absorbed. It can be dependent on temperature but taken as constant in structural fire engineering practice.

Due to the fact that radiation heat transfer is proportional to the difference between the fourth powers of temperatures, problems including radiation boundary conditions require nonlinear algorithms to be solved. Nonlinear solution algorithms will be discussed in Section 2.4.

The heat transfer between surfaces through radiation (cavity radiation) is another form of heat transfer and the heat exchanged between surfaces effect the temperature distribution and, thus, the thermal gradient on the cross-section. This effect is more important for perimeter columns of a structure because they are exposed to fire from one side [6]. As a result of one-sided fire exposure, large thermal gradients occur on perimeter columns. [9] concluded that, large thermal gradients within the cross-section of structural members cause significant thermal stresses; hence change the mechanical behavior of the structural system. Thermally induced moment due to one-sided fire exposure is also shown by [10], [11] and [12].

The heat exchanged between surfaces depend on the optical view of each surface to others. This effect is calculated with view factor F_{ij} , which is the fraction of radiant energy leaving one surface that is intercepted by another surface. To calculate the view factor, area or line integrals are used and generally solved by using numerical integration methods as given in [13], [14].

The view factor calculation performed by FEHEAT will be briefly discussed here and more detailed information can be found on [6]. The formulation for the view factor and the implementation to FEHEAT was verified in [6].

The view factor calculation starts with dividing each element to sub elements. The number of subelements (called as ‘discretize’ within the software and the next chapters in this document) is taken as 6 by default but it can be changed if desired. As the number of subelements increase, the integration for the view factor becomes more accurate.

In Figure 2.1, element i and element j are divided to m and n number of subelements respectively. View factor from subelement m to subelement n (F_{mn}) is calculated using Eq.(2.4a). F_{mn} values are summed over element j and the sum is averaged over the element i to find F_{ij} using Eq.(2.4b).

$$F_{mn} = \frac{1}{2} \cos \theta_{i0,m} \cos \theta_{j0,n} \frac{du_n}{S_{0,m-n}} \quad (2.4a)$$

$$F_{ij} = \frac{1}{m} \sum_m \sum_n F_{mn} \quad (2.4b)$$

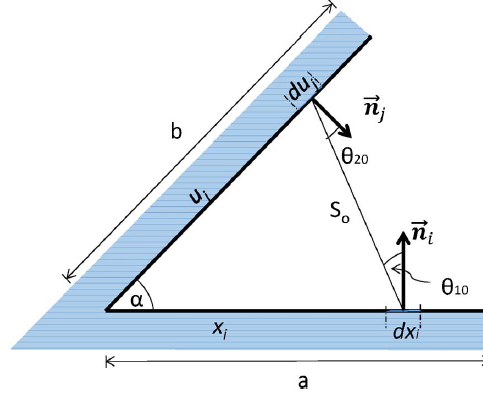


Figure 2.1. View factor calculation [6].

The heat exchange between two surfaces is calculated using Eq.(2.5):

$$q_n = \sigma \varepsilon_{surf} F_{ij} (T_i^4 - T_j^4) \quad (2.5)$$

where q_n is the heat flux due to the surface heat exchange, σ is Stefan-Boltzmann constant, ε_{surf} is the emissivity constant for surface heat exchange and general taken as 1 (i.e., blackbody radiation), T_i and T_j are the surface temperatures in Kelvin. By taking emissivity as 1, it is assumed that no reflection happens between the surfaces in the enclosure [15].

2.2. Finite Element Formulation

In this section, the finite element formulation for the partial differential equations that are used in transient heat transfer analysis will be obtained. Strong form for the governing set of equations considering all possible boundary conditions including convection, radiation due to fire and radiation due to surface heat exchange is given as:

$$-\left(\frac{\partial q_x}{\partial x} + \frac{\partial q_y}{\partial y}\right) = \rho c \frac{\partial T}{\partial t} \quad \text{on } \Omega \quad (2.6a)$$

$$T_s = T_1(x, y, t) \quad \text{on S1} \quad (2.6b)$$

$$q_x n_x + q_y n_y = q_s \quad \text{on S2} \quad (2.6c)$$

$$q_x n_x + q_y n_y = h(T_s - T_{fire}) \quad \text{on S3} \quad (2.6d)$$

$$q_x n_x + q_y n_y = -\sigma \varepsilon_r (T_s^4 - T_{fire}^4) \quad \text{on S4} \quad (2.6e)$$

$$q_x n_x + q_y n_y = -\sigma \varepsilon_{surf} F_{ij} (T_i^4 - T_j^4) \quad \text{on S5} \quad (2.6f)$$

Here ρ and c are the density and the specific heat of the material, respectively. Both properties can be dependent on the temperature of the material, but density changes slowly and generally taken as constant in most practices. On the other hand, the specific heat can change dramatically with temperature and can make sudden peaks, which requires special handling in nonlinear algorithm. For example, specific heat makes a sudden peak at around 735 °C because of metallurgical change for steel.

Five types of boundary conditions; prescribed temperature, prescribed heat flux, convection, radiation due to fire and radiation due to surface heat exchange on surfaces S1, S2, S3, S4 and S5 respectively are shown on a body in Figure 2.2. FEHEAT can handle all five boundary conditions simultaneously for each element. Linear solution is used for prescribed temperature, prescribed heat flux and convection if all material properties are given as constant. When radiation heat flux boundary conditions or temperature dependent material properties exist FEHEAT uses ‘Full Newton-Raphson Method’ for nonlinear solution. Further details are given in Section 2.4.

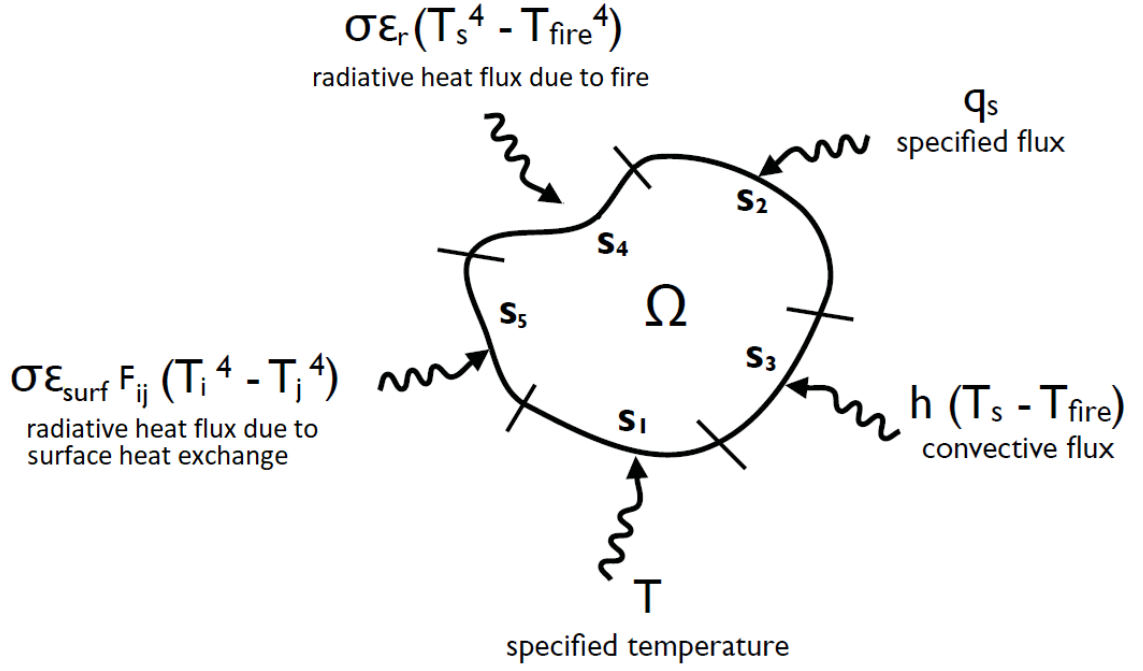


Figure 2.2. Two-dimensional solution domain for general heat transfer in a solid continuum.

The temperatures in finite elements $T^{(e)}$ are approximated with linear piece-wise Lagrange polynomials N_i (shape functions) as in Eq.(2.7a) where i represents each node in an element with a total of r nodes. FEHEAT employs linear 4-node (quadrilateral) isoparametric elements. The shape functions of isoparametric elements are explained in detail by [16].

$$T^{(e)}(x, y, t) = \sum_{i=1}^r N_i(x, y) T_i(t) \quad (2.7a)$$

$$[N(x, y)] = \begin{bmatrix} N_1 & N_2 & N_3 & N_4 \end{bmatrix} \quad (2.7b)$$

$$[B(x, y)] = \begin{bmatrix} \frac{\partial N_1}{\partial x} & \frac{\partial N_2}{\partial x} & \frac{\partial N_3}{\partial x} & \frac{\partial N_4}{\partial x} \\ \frac{\partial N_1}{\partial y} & \frac{\partial N_2}{\partial y} & \frac{\partial N_3}{\partial y} & \frac{\partial N_4}{\partial y} \end{bmatrix} \quad (2.7c)$$

Here, $\{N\}$ is the shape function vector for the four nodes of each element $\Omega_{(e)}$, $[B]$ is the shape function gradient matrix .

The formulation of the ‘Weak Form’ is shown in Eq.(2.8). Here, the mass matrix $[M]$, the heat conduction matrix $[K_c]$ and heat convection matrix $[K_h]$ are defined. Dirichlet (on surface S1) and Neumann (on surface S2) as well as the convective and radiative heat flux (due to fire and surface heat exchange) on the boundary conditions are defined in Eq.(2.8). The convective boundary conditions are treated as a linear problem and the contribution of the convection on the boundary $[K_h]$ is added to the global conduction matrix $[K_c]$ of the solid. This is valid because the convective heat flux depends on the first power of the surface temperature. However, this approach cannot be adopted for radiation boundaries since the heat flux depends on the fourth power of the surface temperature.

$$\left\{ \frac{dT}{dt} \right\} [M] + ([K_c] + [K_h]) \{T\} = \{F_q\} + \{F_{\sigma,rad}\} + \{F_{\sigma,surf}\} + \{F_h\} + \{F_T\} \quad (2.8a)$$

$$[M] = \int_{\Omega_{(e)}} \rho c \{N\} [N] d\Omega_{(e)} \quad (2.8b)$$

$$[K_c] = \int_{\Omega_{(e)}} [B]^T [k] [B] d\Omega_{(e)} \quad (2.8c)$$

$$[K_h] = \int_{S3} h \{N\} [N] d\Gamma \quad (2.8d)$$

$$\{F_T\} = - \int_{S1} (q \cdot \hat{n}) \{N\} d\Gamma \quad (2.8e)$$

$$\{F_q\} = \int_{S2} q_s \{N\} d\Gamma \quad (2.8f)$$

$$\{F_h\} = \int_{S3} h T_{fire} \{N\} d\Gamma \quad (2.8g)$$

$$\{F_{\sigma,rad}\} = - \int_{S4} \sigma \varepsilon_r (T_s^4 - T_{fire}^4) \{N\} d\Gamma \quad (2.8h)$$

$$\{F_{\sigma,surf}\} = - \int_{S5} \sigma \varepsilon_{surf} F_{ij} (T_i^4 - T_j^4) \{N\} d\Gamma \quad (2.8i)$$

2.3. Time Stepping Algorithm

Finite element method is used to solve the temperature distribution for the entire domain for a specific time step. But time stepping is achieved by using the finite dif-

ference method. Thus, Eq.(2.9a) becomes a semi-discrete equation. FEHEAT employs general trapezoidal family of methods which is the most commonly used time stepping algorithm for solving the parabolic heat equation.

$$[M]\{\dot{T}\} + [K]\{T\} = \{F\} \quad (2.9a)$$

$$\{T(0)\} = \{T_0\} \quad (2.9b)$$

Here, the variable $\{T\}$ and $\{\dot{T}\}$ are the temperature and the temperature derivative field vectors. $[M]$ is the mass matrix as defined in Eq.(2.8). $[K]$ is the sum of $[K_c]$ and $[Kh]$ which are defined in Eq.(2.8). $\{F\}$ is the sum of $\{F_q\}$, $\{F_{\sigma,rad}\}$, $\{F_{\sigma,surf}\}$, $\{F_h\}$ and $\{F_T\}$. $\{\dot{T}\}$ is approximated as $\{v\}$ in later equations. The time stepping algorithm starts with the initial temperature field $\{T_0\}$. As shown in Eq.(2.10a), the solution propagates in time depending on the variable α (scalar). Some well-known members of the generalized trapezoidal family are identified in Table 2.1.

$$[M]\{v_{n+1}\} + [K]\{T_{n+1}\} = \{F_{n+1}\} \quad (2.10a)$$

$$\{T_{n+1}\} = \{T_n\} + \Delta t\{v_{n+\alpha}\} \quad (2.10b)$$

$$\{v_{n+\alpha}\} = (1 - \alpha)\{v_n\} + \alpha\{v_{n+1}\} \quad (2.10c)$$

Table 2.1. Trapezoidal families for time stepping algorithm.

Name	α
Forward Euler	0
Crank-Nicolson	0.5
Backward Euler	1

Once the initial temperature field $\{T_0\}$ is known, the initial temperature velocity vector $\{v_0\}$ is evaluated at $t = 0$ as in Eq.(2.11a). Next, the predictor value $\{\tilde{T}_{n+1}\}$ is found using Eq.(2.11b). There are two implementations to predict the next step:

v-form and d-form. The v-form implementation uses the velocity in order to predict the temperature and d-form calculates the temperature field in order to get the velocity field. Both implementations are identical in terms of output but using d-form (which is used by FEHEAT by default) is computationally advantageous when the mass matrix $[M]$ is diagonal.

$$[M]\{v_0\} = \{F_0\} - [K]\{T_0\} \quad (2.11a)$$

$$\{\tilde{T}_{n+1}\} = \{T_n\} + (1 - \alpha)\Delta t\{v_n\} \quad (2.11b)$$

v-form

When v-form is preferred, the velocity vector of the next step $\{v_{n+1}\}$ is calculated by inverting the coefficient matrix as in Eq.(2.12a). Finally, the recursion relation is ended by estimating the temperature field $\{T_{n+1}\}$ of the next step as in Eq.(2.12b) and the iteration is continued to further steps.

$$([M] + \alpha\Delta t[K])\{v_{n+1}\} = \{F_{n+1}\} - [K]\{\tilde{T}_{n+1}\} \quad (2.12a)$$

$$\{T_{n+1}\} = \{\tilde{T}_n\} + \alpha\Delta t\{v_{n+1}\} \quad (2.12b)$$

d-form

When d-form is preferred, the temperature vector of the next step $\{d_{n+1}\}$ is first calculated by inverting the coefficient matrix as in Eq.(2.13a). Finally, the recursion relation is ended by estimating the velocity field $\{v_{n+1}\}$ of the next step as in Eq.(2.13b) and the iteration is continued to further steps.

$$\frac{1}{\alpha\Delta t}([M] + \alpha\Delta t[K])\{T_{n+1}\} = \{F_{n+1}\} + \frac{1}{\alpha\Delta t}[M]\{\tilde{T}_{n+1}\} \quad (2.13a)$$

$$\{v_{n+1}\} = \frac{\{T_{n+1}\} - \{\tilde{T}_{n+1}\}}{\alpha\Delta t} \quad (2.13b)$$

2.4. Nonlinear Solution Algorithm

The heat transfer problem is non-linear due to (1) the radiation boundary conditions at the fire surface, (2) the radiation boundary conditions at the internal cavities (due to surface heat exchange), (3) temperature dependent material properties. For the nonlinear problem, a full Newton-Raphson (NR) iteration scheme is used. N-R requires to assemble the tangent stiffness matrix at each iteration i of each time increment n . The tangent stiffness matrix is also called (and will be referred to in this document) as the Jacobian matrix $[J]$ in the structural engineering practice. Here, only a brief explanation of N-R methodology is provided, and a more detailed explanation can be found in [15].

First, the unbalanced heat vector $\{R\}$ is formed from Eq.(2.13a) (d-form) as defined in Eq.(2.14a). $\{R\}$ is estimated using the temperature field from the previous step $\{T\}$ and the temperature field predictor $\{\tilde{T}\}$. The Jacobian matrix $[J]$ is defined as the derivative of the unbalanced heat load vector as shown in Eq.(2.14b).

$$\{R\} = \frac{1}{\alpha\Delta t} ([M] + \alpha\Delta t[K]) \{T\} - \frac{1}{\alpha\Delta t} [M]\{\tilde{T}\} - \{F\} \quad (2.14a)$$

$$[J] = \frac{\partial R}{\partial T} \quad (2.14b)$$

The contributions to the Jacobian matrix $[J]$ from the radiation vector due to fire $\{F_{\sigma,rad}\}$ and the radiation vector due to surface heat exchange $\{F_{\sigma,surf}\}$ are found using Eq.(2.15c) and Eq.(2.15d) respectively. Here, $\{T\}$ is the surface temperature where the radiation boundary conditions exist, $[J_{rad}]$ and $[J_{surf}]$ are the contributions to the Jacobian matrix due to radiation and surface heat exchange respectively. The sum of $[J_K]$ and $[J_M]$ is simply the global conduction matrix. In the case of linear material properties the global Jacobian matrix is found by adding $[J_{rad}]$ and $[J_{surf}]$ to

the global conduction matrix of the solid body as shown in Eq.(2.15e).

$$[J_K] = [K] \quad (2.15a)$$

$$[J_M] = \frac{1}{\alpha \Delta t} [M] \quad (2.15b)$$

$$[J_{rad}] = 4 \int_{S_4} \sigma \varepsilon_r T^3 \{N\} [N] d\Gamma \quad (2.15c)$$

$$[J_{surf}] = 4 \int_{S_5} \sigma \varepsilon_{surf} F_{ij} T^3 \{N\} [N] d\Gamma \quad (2.15d)$$

$$[J] = [J_K] + [J_M] + [J_{rad}] + [J_{surf}] \quad (2.15e)$$

Another source of nonlinearity arises when a temperature dependent material property exists. Material properties that effect the heat transfer problem in general are the thermal conductivity coefficient (k), the specific heat (c) and the density (ρ).

In the case of temperature dependent thermal conductivity, $[K]$ is no longer constant throughout time history and this results in additional contribution to $[J_K]$. As can be seen from the Eq.(2.16), the resultant Jacobian matrix due to nonlinear conductivity $[J_{K,NL}]$ is an asymmetric matrix after addition of these terms:

$$[J_{K,NL}] = [K] + \int_{\Omega(e)} [B]^T \frac{dk}{dT} \nabla(T) [N] d\Omega(e) \quad (2.16)$$

Considering the fact that the thermal conductivity usually varies slowly with temperature, these additional terms are expected to be very small. Thus, to avoid an asymmetric tangent matrix, the additional terms due to nonlinearity in thermal conductivity are neglected and $[J_K]$ is used instead of $[J_{K,NL}]$ while assembling for the global Jacobian matrix in FEHEAT. This is also suggested by [17] and [18] to obtain a more efficient solution algorithm.

The volumetric heat capacity (that is the product ρc) can also change with temperature. In this case the mass matrix $[M]$ is no longer constant and $[J_M]$ is replaced

by $[J_{M,NL}]$ which is calculated using Eq.(2.17):

$$[J_{M,NL}] = \frac{1}{\alpha \Delta t} [M] + \frac{1}{\alpha \Delta t} \int_{\Omega(e)} \frac{\partial(\rho c)}{\partial T} \{N\} [N] \left(\{T\} - \{T_n\} - \frac{\Delta t}{1 - \alpha} \{v_n\} \right) d\Omega_{(e)} \quad (2.17)$$

where $\{T_n\}$ and $\{v_n\}$ are the temperature and the velocity vectors for the previous step and $\{T\}$ is the temperature vector estimated for the next step.

The global Jacobian matrix considering all types of nonlinearities including radiation due to fire, radiation due to surface heat exchange, nonlinearity in the volumetric heat capacity is assembled as shown in Eq.(2.18).

$$[J] = [J_K] + [J_{MNL}] + [J_{rad}] + [J_{surf}] \quad (2.18)$$

Once the global Jacobian matrix is assembled, N-R algorithm is performed as below at step n to determine the temperature in the next time step until a specified tolerance value (TOL in Figure 2.3) is reached:

$$\{\Delta T_{n+1}^{i+1}\} = [J_{n+1}^i]^{-1} \{-R_{n+1}^i\} \quad (2.19a)$$

$$\{T_{n+1}^{i+1}\} = \{T_{n+1}^i\} + \{\Delta T_{n+1}^{i+1}\} \quad (2.19b)$$

The matrix assembly and time stepping algorithm of FEHEAT are shown in Figure 2.3. This flowchart shows that the Jacobian matrix is updated at each iteration in each time increment Δt . The N-R solution algorithm is only triggered if the user specifies radiative boundary conditions or nonlinear material properties, otherwise Eq.(2.12a) or Eq.(2.13a) are used instead of Eq.(2.19). This algorithm was first created in [5]. The modifications to the algorithm that have been made within this study are shown in red.

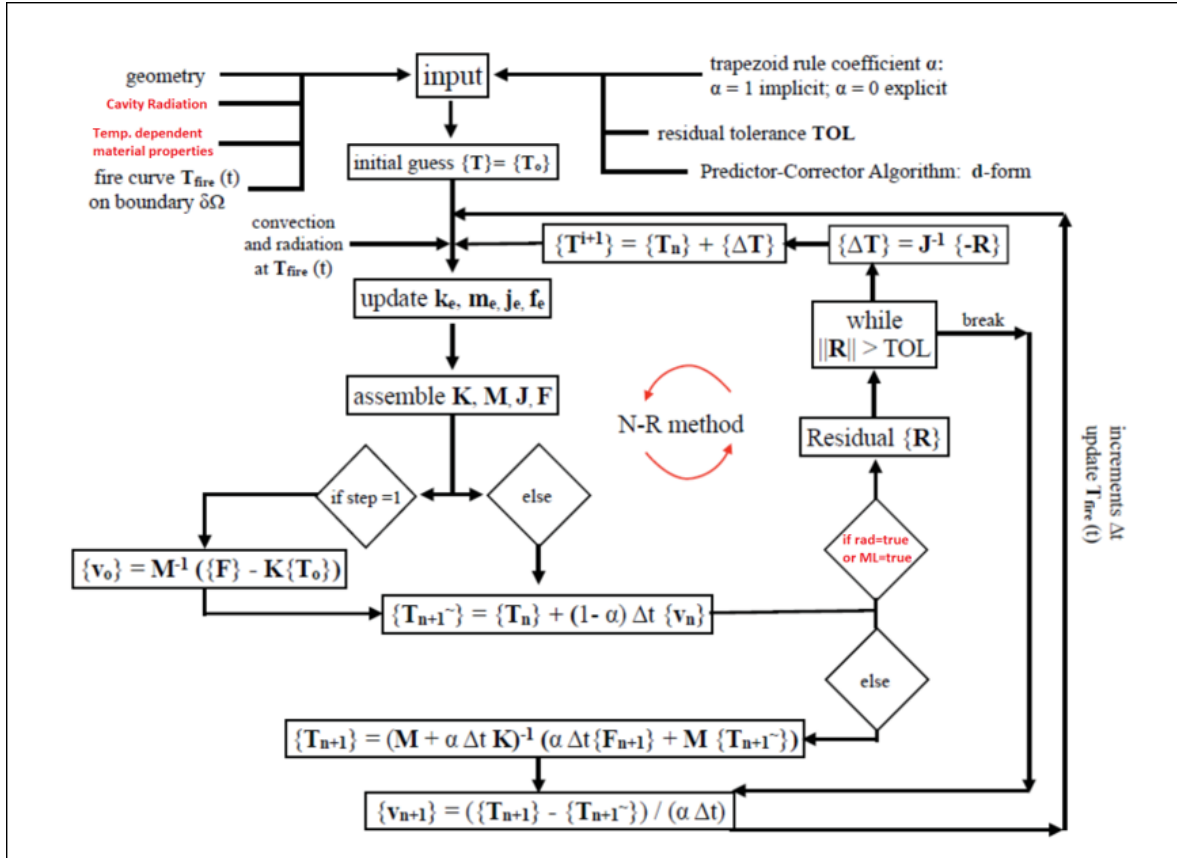


Figure 2.3. Flowchart of the FEHEAT algorithm for linear and nonlinear transient heat transfer problem [5].

2.5. Capabilities and Limitations

FEHEAT is a finite element code that is currently capable of solving two-dimensional transient heat transfer problems in solids with convective and radiative boundary conditions. Further, a constant or varying temperature or heat flux can be specified on the boundaries.

The code can solve problems including cavity radiation (heat exchange between surfaces). View factor calculation is performed for each cavity within the cross-section and the tangent matrix is modified as necessary.

FEHEAT uses $\alpha = 1$ which means that the heat transfer problem is fully implicit. Advantages of using explicit and implicit algorithms are explained in detail by [16]. Implicit algorithms are unconditionally stable and no stability checks for the determination of the time step is required. Note that ABAQUS software which was used to verify FEHEAT results also use implicit algorithms as default.

FEHEAT adopts the full Newton-Raphson nonlinear algorithms to solve nonlinearities due to (1) radiation on the boundary due to fire, (2) radiation heat exchange between surfaces when cavities exist on the cross-section and (3) material nonlinearities when a material property is given as temperature dependent. The algorithm is robust and FEHEAT switches nonlinear and linear algorithms upon the user input. Newton-Raphson algorithm has converged and been very accurate for the verification problems stated in Chapter 3, not more than six iterations per time increment is needed to converge to a solution for most of the problems.

Currently, FEHEAT is not capable of simulating three-dimensional heat transfer problems but is designed such that expansion to the third dimension is both easily and likely to be done in the near future. However, such problems are not validated and expanding to three dimensions is not a focus in this study. Such implementation will require a relatively more study on graphical user interface.

With the use of the parametric modelling interface that is specifically designed for modelling multiple models based on parameters in a single menu, FEHEAT provides a powerful tool for parametric studies. FEHEAT also has batch analysis feature, which enables multiple models to be run all at once.

FEHEAT has extensive libraries for cross-sections, materials, insulation materials and fire curves. All libraries can be further expanded by the user as desired.

3. VALIDATION

3.1. Validation for Rectangular Concrete

FEHEAT is first validated for a typical problem, in which a rectangular concrete column is heated from all four sides with standard ISO 834 fire. Eurocode 2 [8] provides temperature distributions for this specific problem for columns with varying dimensions in appendix E of the standard. Since the data provided are given as field results, the comparisons will also be made on field results.

Same problem is modeled and calculated using FEHEAT and ABAQUS. Note that all parameters and assumptions mentioned below are the same as given in [8].

A square concrete column with dimensions of 300 mm to 300 mm was heated for 120 min from all four sides as shown in Figure 3.1. Both radiation and convection boundary conditions were defined for all fire sides. Emissivity ε was taken as 0.7 and the convection factor h_c was taken as 25 W/m²K. Time increment (Δt) was taken as 60 secs.

The lower limit of thermal conductivity of concrete was used as follows:

$$k = 1.36 - 0.136(T/100) + 0.0057(T/100)^2 \quad \text{for } 20^\circ\text{C} \leq T \leq 1200^\circ\text{C} \quad (3.1)$$

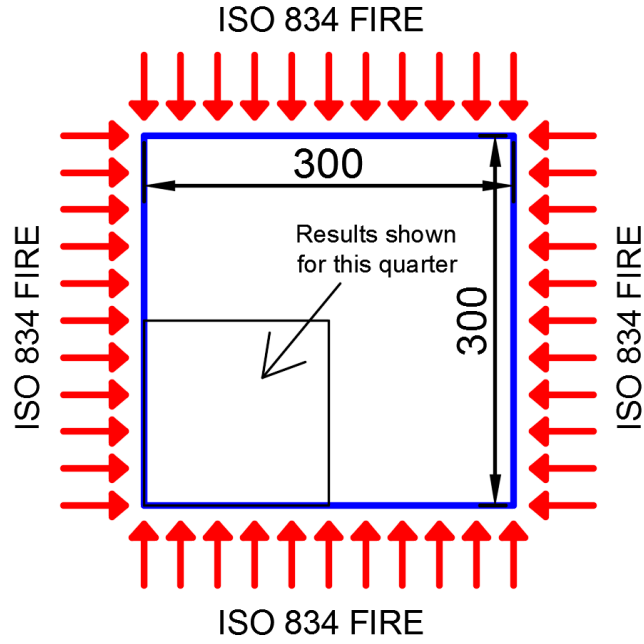


Figure 3.1. Sketch of the model for the rectangular column.

The specific heat of concrete with moisture content of 1.5% was used as follows:

$$c(T) = 900 \text{ (J/kgK)} \quad \text{for } 20^\circ\text{C} \leq T \leq 100^\circ\text{C} \quad (3.2a)$$

$$c(T) = 1470 \text{ (J/kgK)} \quad \text{for } 100^\circ\text{C} < T \leq 115^\circ\text{C} \quad (3.2b)$$

$$c(T) = 1470 - 470 \left(\frac{(T - 115)}{85} \right) \text{ (J/kgK)} \quad \text{for } 115^\circ\text{C} < T \leq 200^\circ\text{C} \quad (3.2c)$$

$$c(T) = 1000 + (T - 200)/2 \text{ (J/kgK)} \quad \text{for } 200^\circ\text{C} < T \leq 400^\circ\text{C} \quad (3.2d)$$

$$c(T) = 1100 \text{ (J/kgK)} \quad \text{for } 400^\circ\text{C} < T \leq 1200^\circ\text{C} \quad (3.2e)$$

Density was also taken as temperature dependent as follows:

$$\rho(T) = 2300 \text{ (kg/m}^3\text{)} \quad \text{for } 20^\circ\text{C} \leq T \leq 115^\circ\text{C} \quad (3.3a)$$

$$\rho(T) = 2300(1 - 0.02(T - 115)/85) \text{ (kg/m}^3\text{)} \quad \text{for } 115^\circ\text{C} < T \leq 200^\circ\text{C} \quad (3.3b)$$

$$\rho(T) = 2300(0.98 - 0.03(T - 200)/200) \text{ (kg/m}^3\text{)} \quad \text{for } 115^\circ\text{C} < T \leq 400^\circ\text{C} \quad (3.3c)$$

$$\rho(T) = 2300(0.95 - 0.07(T - 400)/800) \text{ (kg/m}^3\text{)} \quad \text{for } 400^\circ\text{C} < T \leq 1200^\circ\text{C} \quad (3.3d)$$

The standard temperature-time curve as defined in Eurocode 2 [8] was used, which is calculated as follows:

$$T_{fire} = 20 + 345 \log_{10}(8t + 1) \quad (3.4)$$

The temperature contours provided by Eurocode 2 [8] and the results obtained by FEHEAT and ABAQUS models are provided for one quarter of the column in Figure 3.2. It can be seen that all three temperature distributions almost exactly match each other.

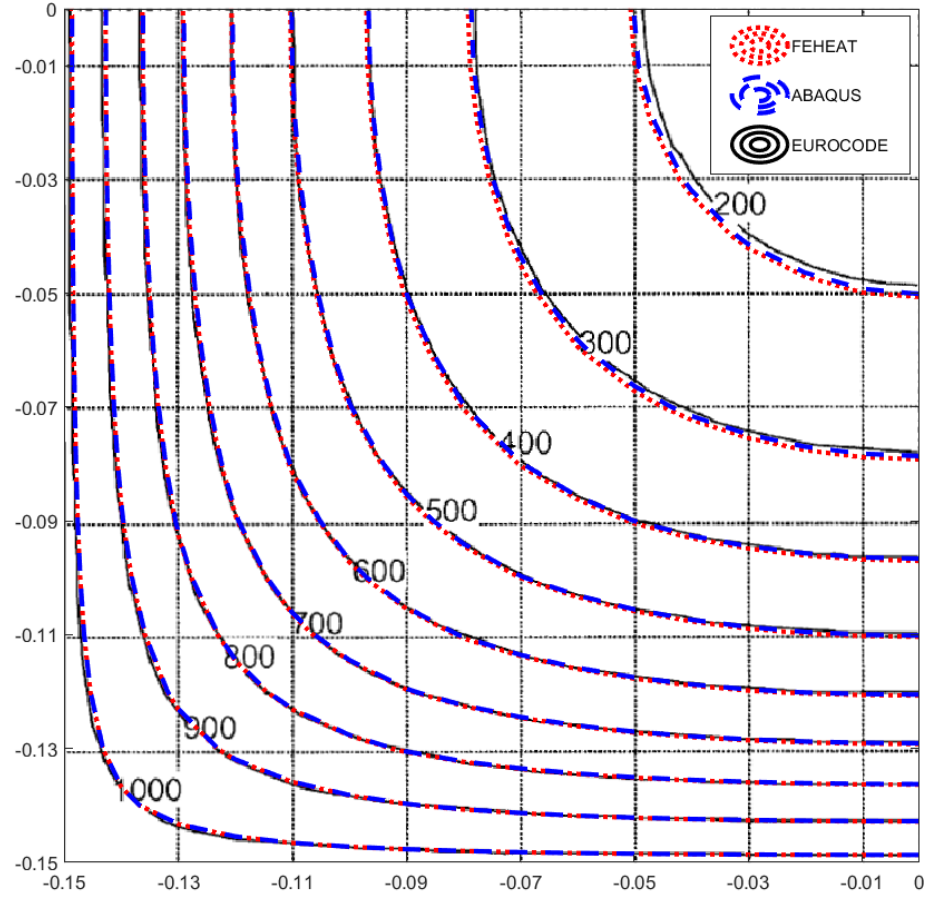


Figure 3.2. Comparison of temperature distributions obtained using FEHEAT and ABAQUS with Eurocode 2 data.

3.2. Validation with Commercial Finite Element Software ABAQUS

FEHEAT was verified with widely used, general-purpose finite element software ABAQUS. All verifications in this chapter are made for steel cross-sections.

First, validations for common case scenarios were determined considering fire exposure from the bottom of the surface with radiation and convection boundary conditions for each cross-section types that are supported by FEHEAT. Cavity radiation was enabled for the common case scenario for all cross-sections except box section. For I-shape both linear and nonlinear material cases are considered whereas for other cross-section types, only nonlinear material is considered.

Table 3.1. A summary of verification studies.

Study Description	Cross-Section Class	Material	Ins	Surf	Rad	Conv	Cold
Validation for common case with linear material	I-Shape (thin) and I-Shape (thick)	Linear	X	X	✓	✓	X
Validation for common case	I-Shape (thin), I-Shape (thick), Angle, Channel and T-Shape	Nonlinear	X	✓	✓	✓	X
Validation for common case	Box	Nonlinear	X	X	✓	✓	X
Insulation validation	I-Shape (thin)	Nonlinear	✓	X	✓	✓	X
Convection-cold surface validation	I-Shape (thin)	Nonlinear	X	X	X	✓	✓

Also, validations for convection-only case and insulated case were also made. In Table 3.1, a summary of the validations performed within this section is provided. ‘Ins’, ‘Surf’, ‘Rad’, ‘Conv’, ‘Cold’ columns refer to insulation, surface heat exchange, radiation from bottom flange or top flange, convection (from bottom or top flange) and cold surface assigned at the top flange respectively. Further explanations are made in related sections. All cross-section properties are given in Table 3.2.

Table 3.2. Cross-section properties.

Cross-section Name	Section depth (mm)	Section width (mm)	Flange thickness (mm)	Web thickness (mm)
I-Shape (thin)	300	300	10	10
I-Shape (thick)	400	200	50	30
Box	300	200	10	10
Angle	150	150	10	10
Channel	300	200	10	10
T-Shape	300	200	10	10

3.2.1. Common Case with Linear Material Properties

Verification for a common case that includes radiation and convection boundary conditions from one side of the cross-section is examined first with linear material properties considering cavity radiation.

Verification studies presented in this section were conducted using linear material properties of steel. The thermal conductivity coefficient k was taken as 45 W/m.K. The specific heat capacity c was taken as 600 J/kgK. Finally, the density was taken as 7850 kg/m³.

The surface was heated from the bottom surface of the bottom flange using convective and radiative boundary conditions with ISO834 fire as defined in Eurocode. Convection heat transfer coefficient h_v was taken as 25 W/m²K. Emissivity coefficient was taken as 0.7 as given in Eurocode 3 [19] and commonly used for steel surface.

Heat exchange between surfaces was taken into account in both FEHEAT and ABAQUS models. The effect of this can be clearly seen from the graphs (especially for thin case) where top flange temperature reaches even greater values than web temperature in later time steps. This would not be possible without considering the heat exchange between surfaces.

Two hypothetical I-shape cross-sections that are representing two extreme cases in terms of the thickness of the solid shape were defined. They are named simply as I-Shape (thin) and I-Shape (thick) throughout this study. I-Shape (thin) cross-section is used in further verifications for parameters like insulation and convection in next sections.

A summary of the analysis parameters is given in Table 3.3. The comparisons are made for I-Shape (thin) and I-Shape (thick) in Figure 3.3 and Figure 3.4 respectively. The cross-section properties are given in Table 3.2.

Table 3.3. Analysis parameters for linear case.

Parameter Name	Value
Cross-section	I-Shape (thin), I-Shape (thick)
Material	Steel
Fire curve	ISO 834
Thermal conductivity coefficient, k (W/m.k)	45
Specific heat, c (J/kgK)	600
Density, ρ (kg/m ³)	7850
Convection heat transfer coefficient, h_v (W/m ² K)	25
Emissivity coefficient for surfaces exp. to fire, ε_{rad}	0.7
Emissivity coefficient for cavity radiation, ε_{surf}	1.0
Time increment, Δt (secs)	60

It can be seen from the comparisons that FEHEAT results almost perfectly fits the results obtained using ABAQUS. Also notice that for I-Shape (thin) Node3 (which is at the top of the top flange) experiences greater temperatures than Node2 (which is at the center of the web) as it can be seen in Figure 3.3. This is as a result of the fact that the surface heat exchange between the top and bottom flange is much faster than the heat exchange between the web and the bottom flange. The difference between the heat exchanges is because the optical view of the bottom flange is better to the top flange than it is to the web which results in greater view factors and, thus, greater heat flux.

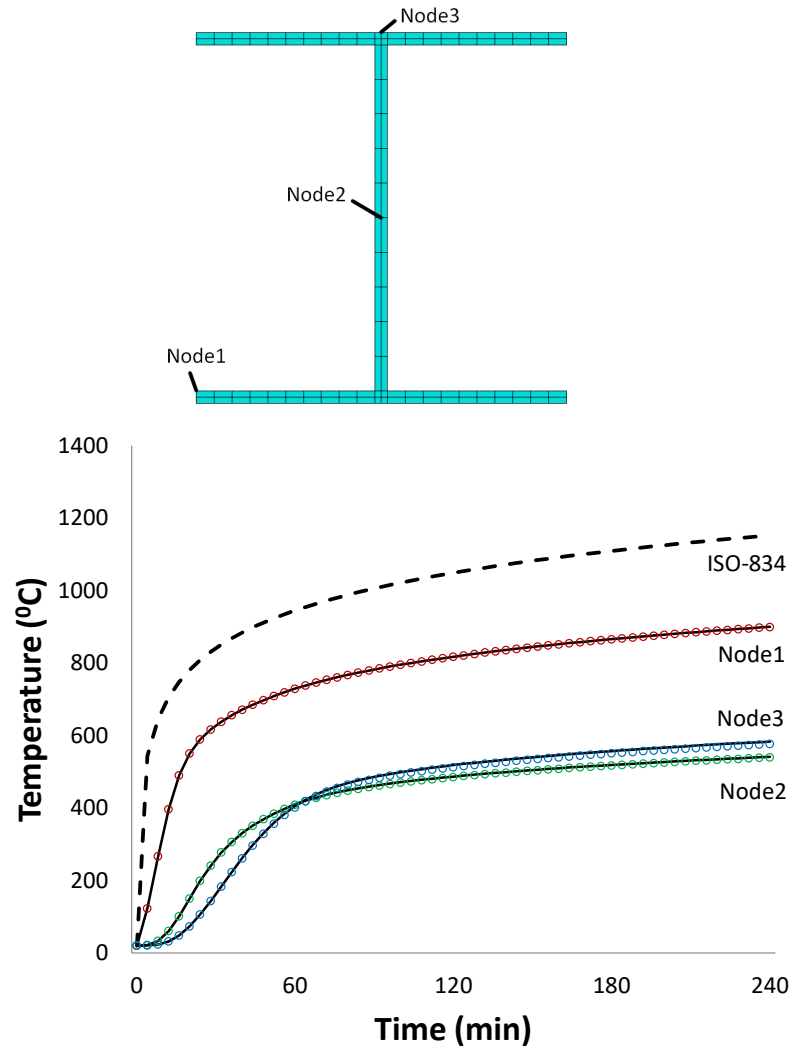


Figure 3.3. Common case with I Shape (thin) and linear material properties (solid lines represent ABAQUS results, circle marks represent FEHEAT results).

For I-Shape (thick) case, the temperature at the top surface of the bottom flange is less than it is for I-Shape (thin). This results in cavity radiation (surface heat exchange) being less effective and Node2 experiences greater temperatures than Node3 (Figure 3.4).

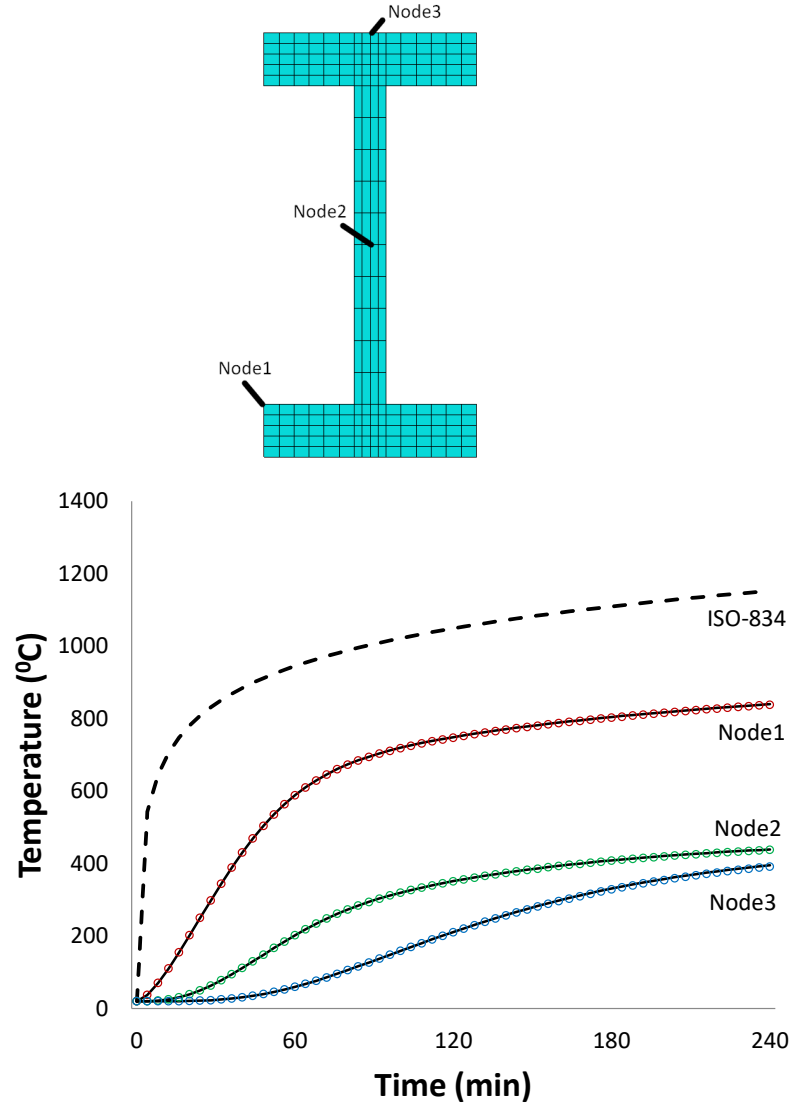


Figure 3.4. Common case with I Shape (thick) and linear material properties (solid lines represent ABAQUS results, circle marks represent FEHEAT results).

3.2.2. Common Case with Nonlinear Material Properties

In this section, Verification for a common case that includes radiation and convection boundary conditions from one side of the cross-section is examined with nonlinear material properties considering cavity radiation.

Verification studies presented in this section were conducted using nonlinear material properties of steel. The changes of the thermal conductivity coefficient k and the specific heat capacity c of steel with temperature are given in Figure 3.5 and Figure 3.6. Notice the sudden peak of the specific heat at around 735 degrees. This sudden peak possesses a challenge for nonlinear solution algorithms. Finally, the density ρ was considered constant and taken as 7850 kg/m³. A summary of the analysis parameters for nonlinear case is given in Table 3.4.

Table 3.4. Analysis parameters for nonlinear case.

Parameter Name	Value
Cross-section	All types
Material	Steel (nonlinear)
Fire curve	ISO 834
Thermal conductivity coefficient, k (W/mK)	Temp.-dependent
Specific heat, c (J/kgK)	Temp.-dependent
Density, ρ (kg/m ³)	7850
Convection heat transfer coefficient, h_v (W/m ² K)	25
Emissivity coefficient for surfaces exp. to fire, ε_{rad}	0.7
Emissivity coefficient for cavity radiation (if applicable), ε_{surf}	1.0
Time increment, Δt (secs)	60

All boundary conditions and assumptions other than material properties are the same as the linear case that is described in the previous section. One exception is that T-Shape was exposed to the fire from the top of the top flange which is not an actual exception. Another exception is that the surface heat exchange was not considered for box shape.

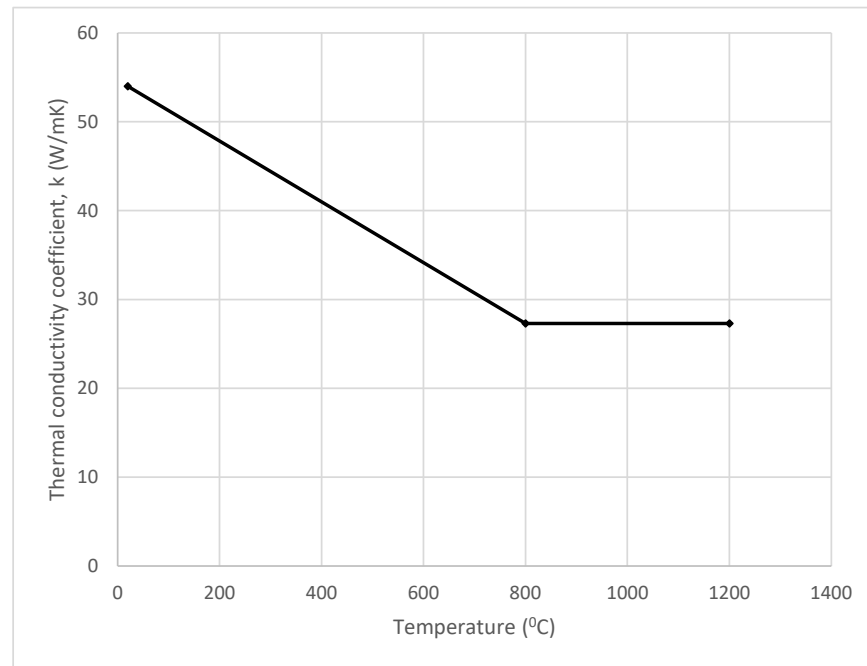


Figure 3.5. Change of thermal conductivity coefficient of steel with temperature.

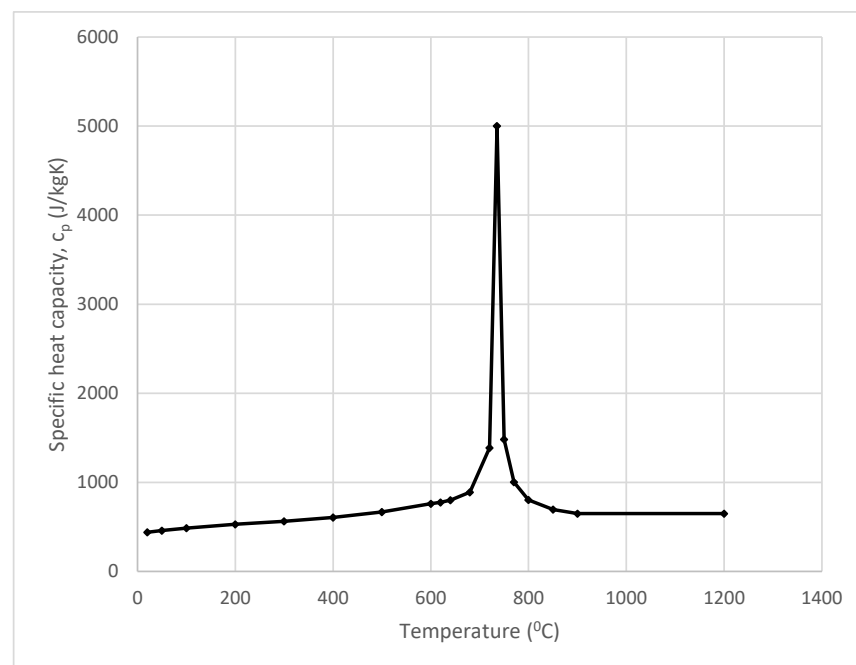


Figure 3.6. Change of specific heat capacity of steel with temperature.

Below the comparisons are made for I-Shape (thin), I-Shape (thick), angle, channel and T-Shape in Figures 3.3 and Figures 3.7, 3.8, 3.9, 3.10, 3.11, 3.12 respectively. The cross-section properties are given in Table 3.2. It can be seen from the comparisons that FEHEAT results, again, almost perfectly fits the results obtained using ABAQUS.

In Figure 3.7 for I-Shape (thin), Node3 reaches greater temperatures than Node2 as it was in the linear case due to the cavity radiation. For Node1, a sudden change in the slope of the curve can be clearly seen when the temperature reaches around 735 degrees. This is due to the sudden change of the specific heat as shown in Figure 3.6 at that interval temperatures.

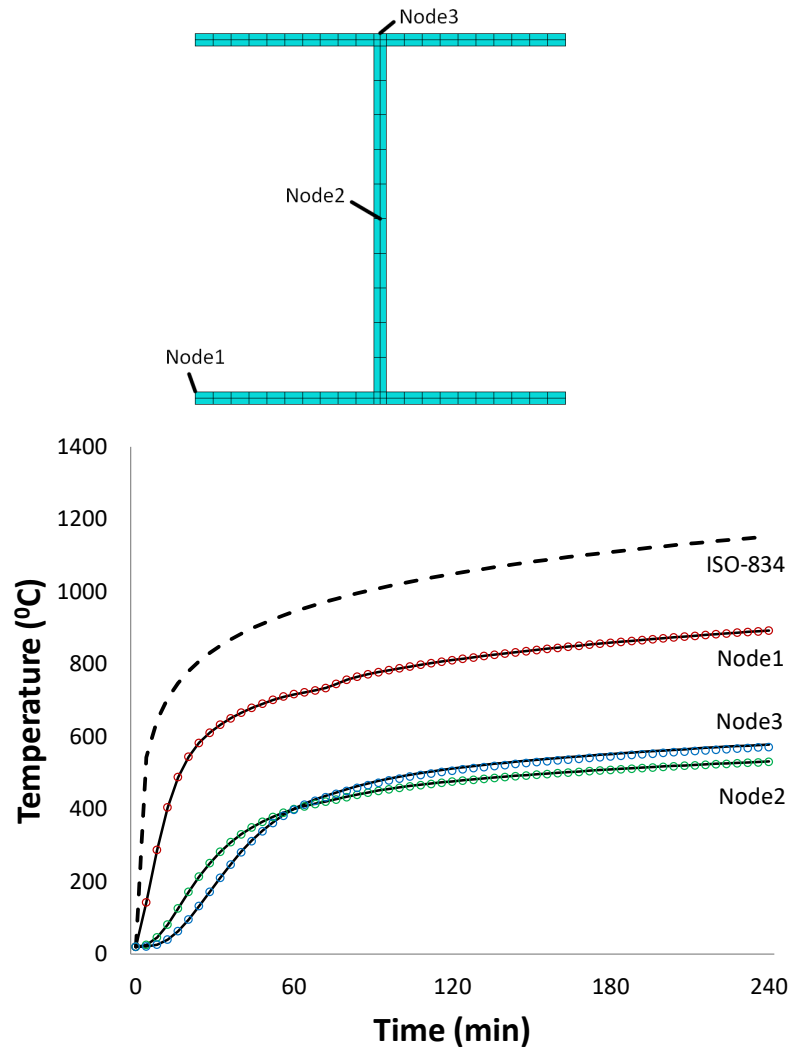


Figure 3.7. Common case with I Shape (thin) and nonlinear material properties (solid lines represent ABAQUS results, circle marks represent FEHEAT results).

In Figure 3.8 for I-Shape (thick), the effects of both cavity radiation and sudden change in the specific heat are seen less. This is because the temperature at the top of the bottom flange reaches considerably high values at very late steps due to the very thick flange. Notice that when the temperature at Node1 reaches 735 degrees, the slope of ISO 834 fire curve almost flat and this results in a relatively smooth curve for Node1.

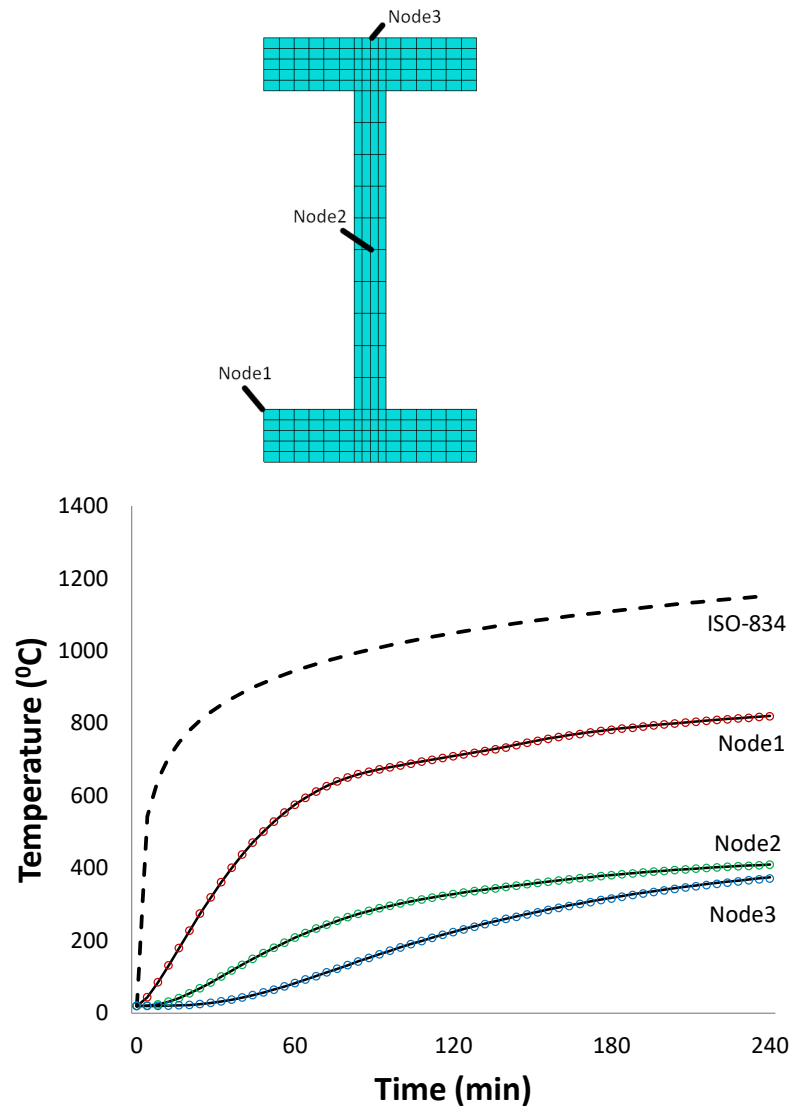


Figure 3.8. Common case with I Shape (thick) and nonlinear material properties (solid lines represent ABAQUS results, circle marks represent FEHEAT results).

For the box section, the heat flows only through the webs which are at the sides of the cross-section to reach the top flange because the cavity radiation for this model is not allowed. This results in high temperatures at the corner of the bottom flange (Node1 in Figure 3.9). Notice that Node2 has greater temperature than Node3. This is expected because the heat must go through the web to reach the top flange.

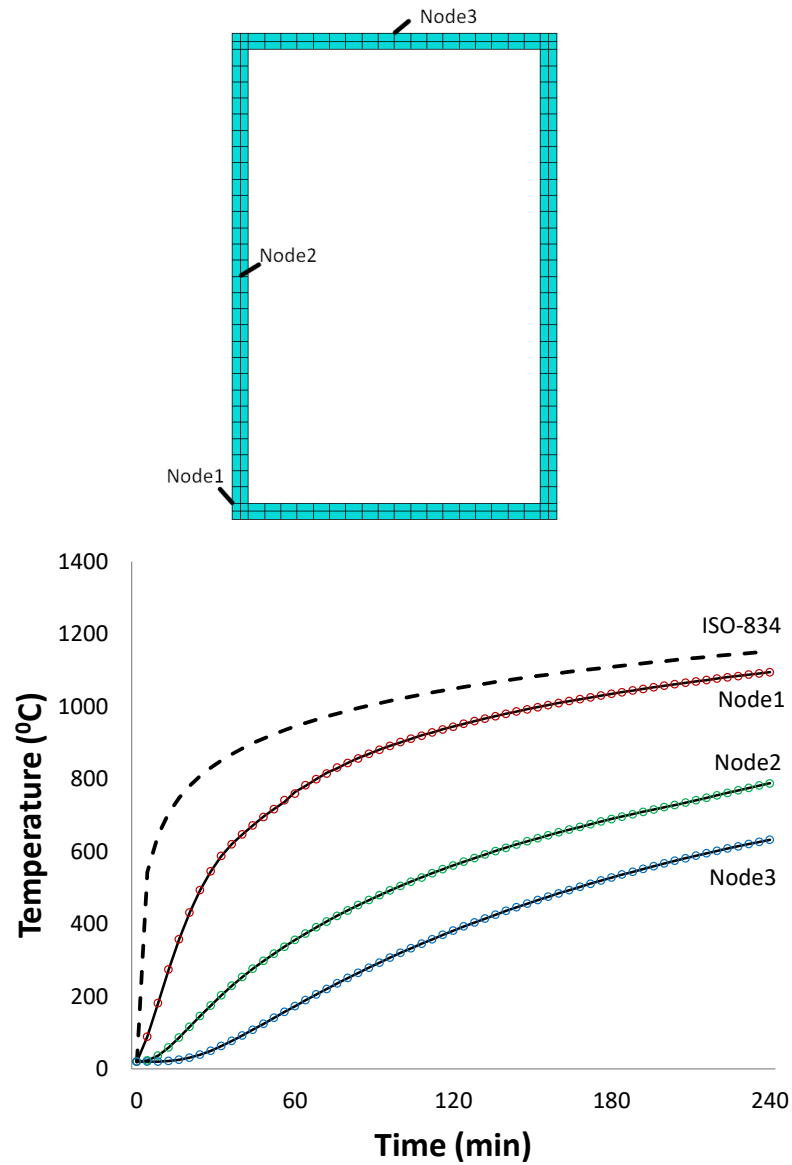


Figure 3.9. Common case with box section and nonlinear material properties (solid lines represent ABAQUS results, circle marks represent FEHEAT results).

The temperature curves for angle section (Figure 3.10) also show the effects of the sudden change in the specific heat for Node1. Also, it can be said that cavity radiation still plays some role in heat transfer but heat transfer through surface heat exchange is slow because the optical view of the two sides is relatively less since the two sides are perpendicular to each other.

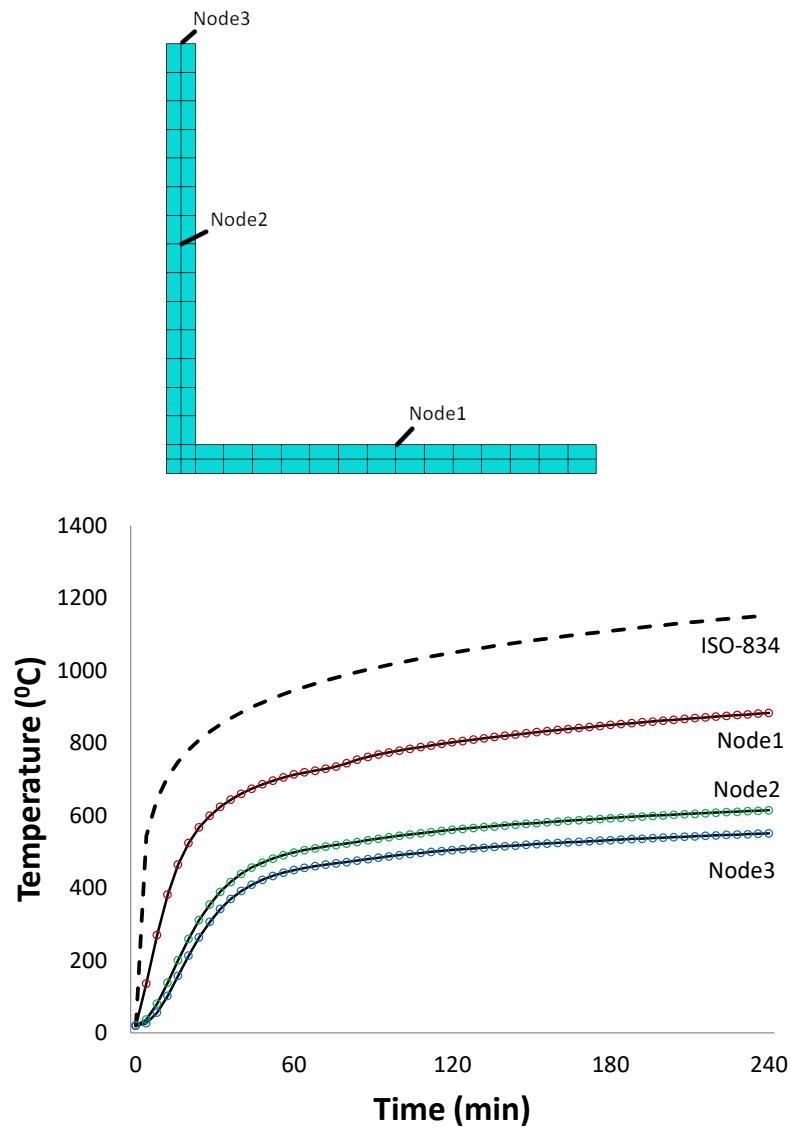


Figure 3.10. Common case with angle section and nonlinear material properties (solid lines represent ABAQUS results, circle marks represent FEHEAT results).

The temperature curves for channel section (Figure 3.11) look similar to the I-Shape (thin) case (see Figure 3.7). The effects of both cavity radiation and sudden change in the specific heat on the temperature distribution are seen clearly.

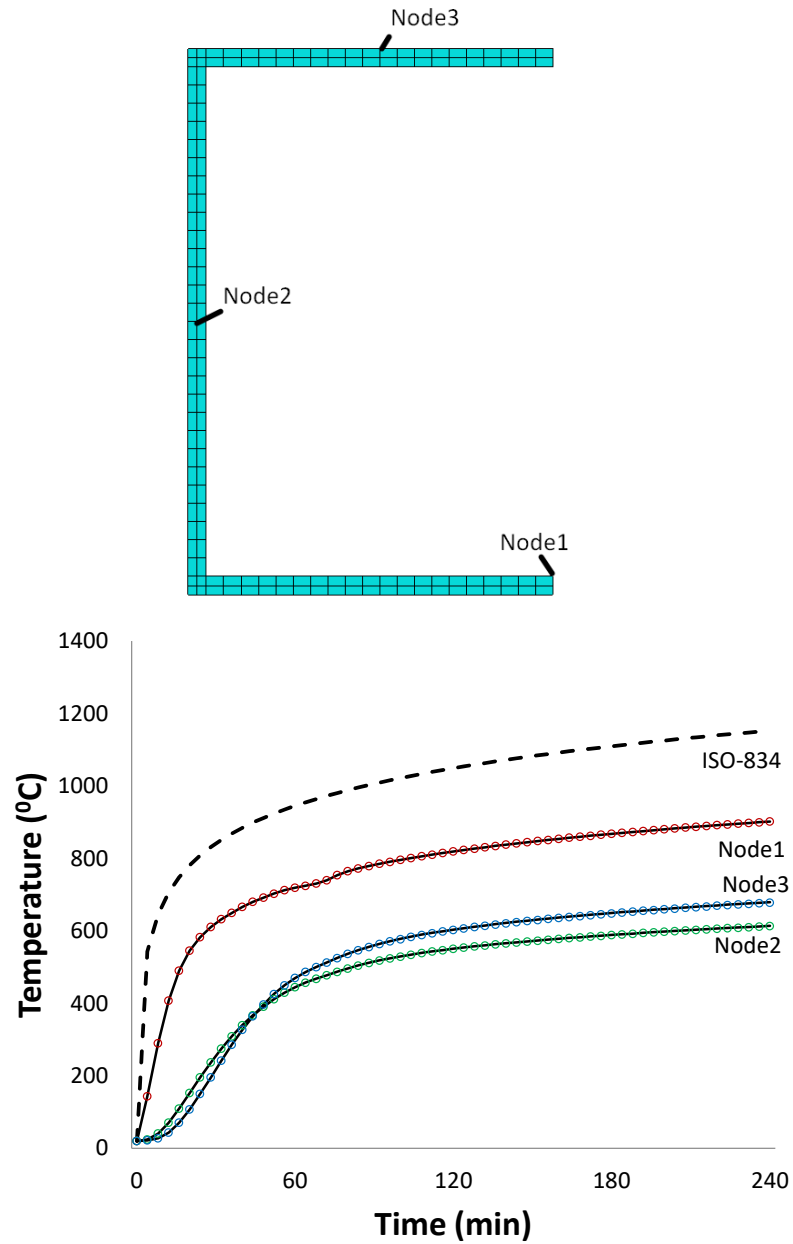


Figure 3.11. Common case with channel section and nonlinear material properties (solid lines represent ABAQUS results, circle marks represent FEHEAT results).

The temperature curves for T-Shape (Figure 3.12) look similar to the angle case (see Figure 3.10). The effect of cavity radiation is seen less as it was for angle section.

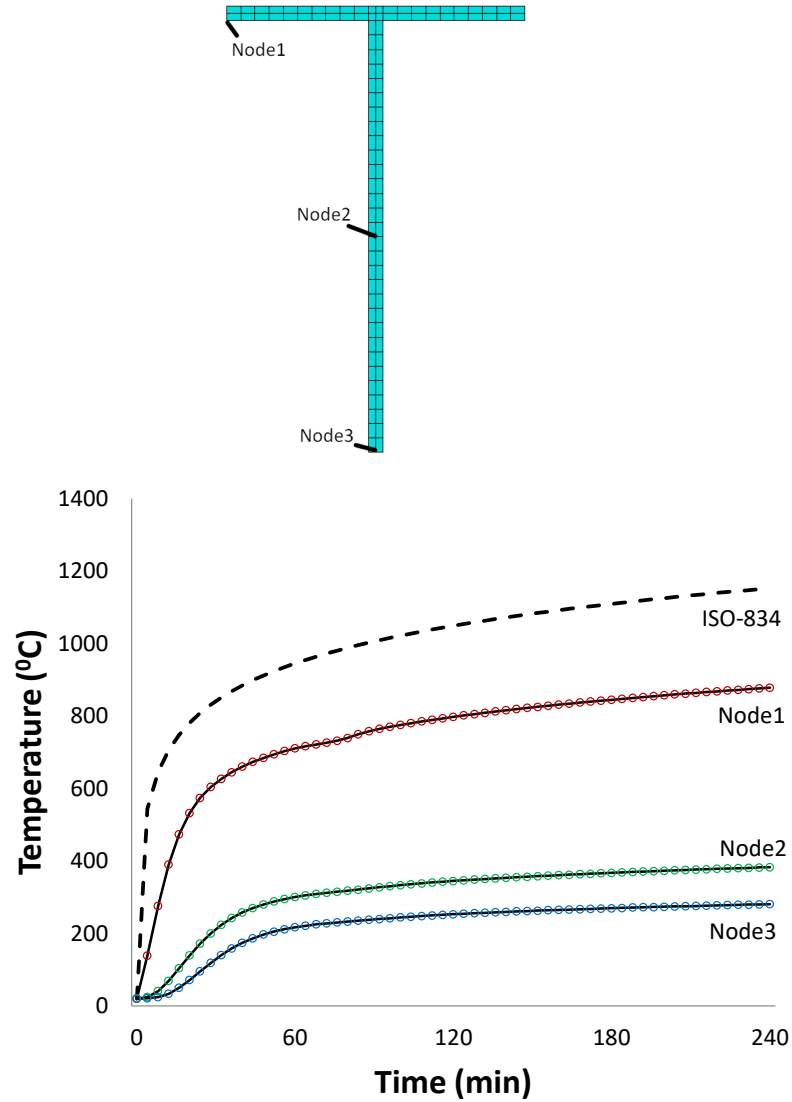


Figure 3.12. Common case with T-Shape and nonlinear material properties (solid lines represent ABAQUS results, circle marks represent FEHEAT results).

3.2.3. Insulation Verification

Verifications up to this section did not include the case when insulation is applied to a surface of the cross-section. In this section, a similar case to the common case that is described above with the bottom flange insulated is considered for this verification.

Bottom flange is heated and insulated from sides as well. Note that surface heat exchange (which is already verified in above cases) is not enabled to see a clear effect of the insulation to the accuracy of the FEHEAT results. All steel material properties are as described above for nonlinear case. Insulation material is Gypsum Board for which the thermal conductivity coefficient k is $0.2W/m.K$, the specific heat capacity c is $1700J/kgK$ and the density ρ is $800kg/m^3$.

Table 3.5. Analysis parameters for insulated case.

Parameter Name	Value
Cross-section	I-Shape (thin)
Material	Steel (nonlinear)
Fire curve	ISO 834
Thermal conductivity coefficient, k (W/mK)	Temp.-dependent
Specific heat, c (J/kgK)	Temp.-dependent
Density, ρ (kg/m ³)	7850
Convection heat transfer coefficient, h_v (W/m ² K)	25
Emissivity coefficient for surfaces exp. to fire, ε_{rad}	0.7
Emissivity coefficient for cavity radiation, ε_{surf}	1.0
Time increment, Δt (secs)	60

Analysis parameters for insulated case are given in Table 3.5. The results are presented in Figure 3.13. It can be seen that temperature at Node1 reaches very high values since it is placed just after the insulation.

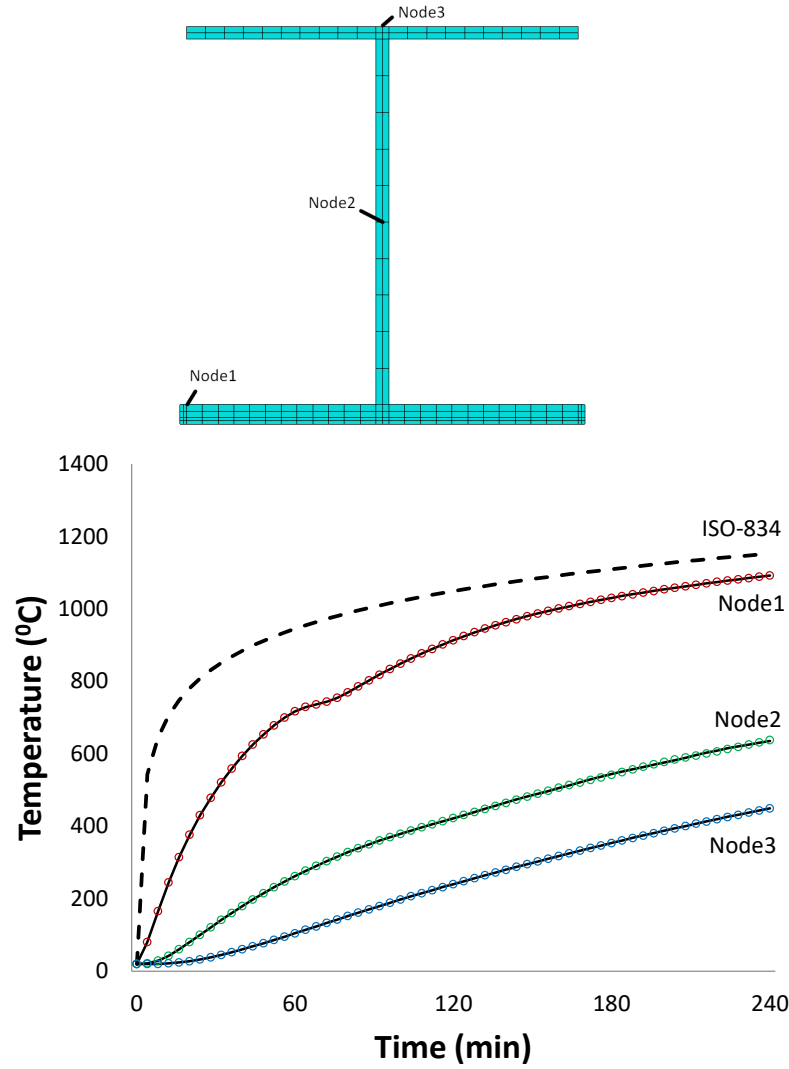


Figure 3.13. Insulated case with I-Shape (thin) (solid lines represent ABAQUS results, circle marks represent FEHEAT results).

3.2.4. Convection Verification

The effect of convection is known to be less than radiation in most problems. Thus, an additional verification was made for the case when only convection boundary conditions exist.

Verification was made again using I-Shape (thin). The cross-section is heated from the bottom of the bottom flange with ISO834 fire considering only convection

and ignoring radiation. Surface heat exchange is also not considered in order to see the effect of convection boundaries clearly. Convection heat transfer coefficient h_v was taken as 25 W/m²K.

A cold (cooling) surface was defined at the top surface of the top flange as well. Convection heat transfer coefficient h_v is taken as 9 W/m²K as suggested by Eurocode 1 [20]. Ambient temperature is taken as 20 degrees. The analysis parameters for convection-only case are given in Table 3.6. The results are shown in Figure 3.14. It

Table 3.6. Analysis parameters for convection-only case.

Parameter Name	Value
Cross-section	I-Shape (thin)
Material	Steel (nonlinear)
Fire curve	ISO 834
Thermal conductivity coefficient, k (W/mK)	Temp.-dependent
Specific heat, c (J/kgK)	Temp.-dependent
Density, ρ (kg/m ³)	7850
Convection heat transfer coefficient(fire-exposed), h_v (W/m ² K)	25
Convection heat transfer coefficient(cold), h_v (W/m ² K)	9
Time increment, Δt (secs)	60

can be seen that Node3 stays at very low temperatures (just above 200 degrees) even after 4 hours. This is due to both the cooling at the top flange and the cavity radiation being not permitted.

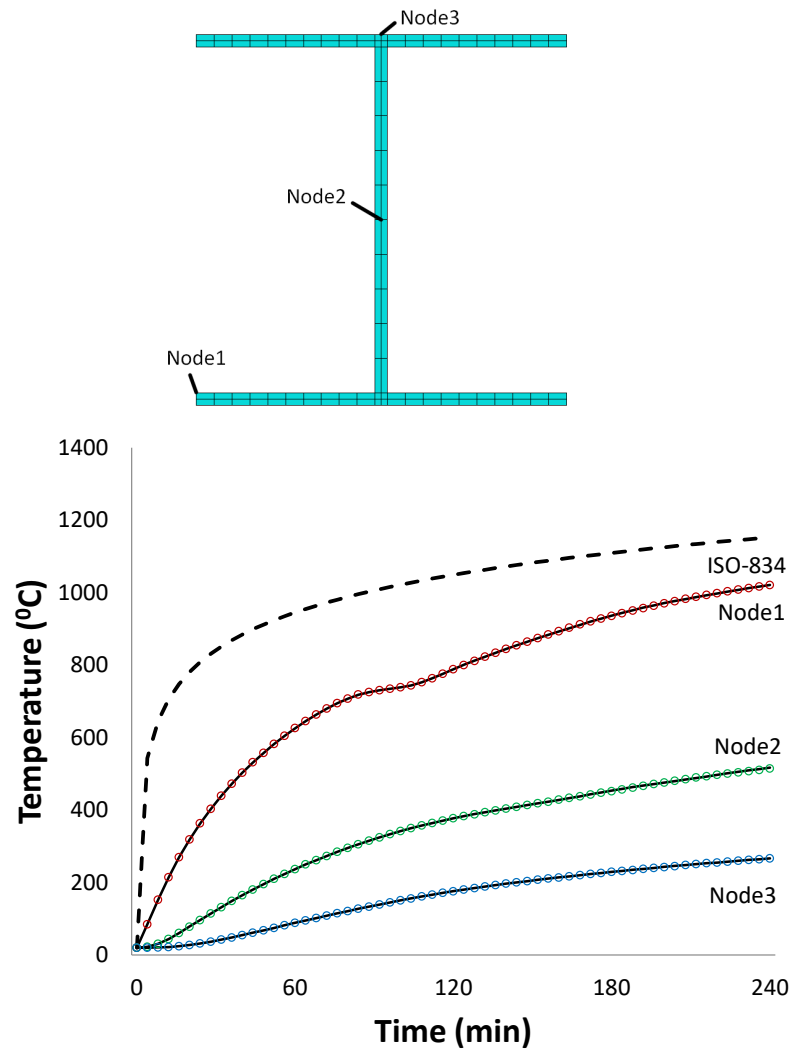


Figure 3.14. Convection-only case with I-Shape (thin) (solid lines represent ABAQUS results, circle marks represent FEHEAT results).

4. GRAPHICAL USER INTERFACE (GUI)

Speeding up the modelling phase is one of the main focuses in this study. A user-friendly interface is crucial to accomplish this target. All menus are designed to be as simple as possible. GUI creates all the input for FEHEAT and provides post-processing tools as well. By providing plots and error checks from the user data as the user gives the input, it is aimed to minimize the mistakes from user inputs.

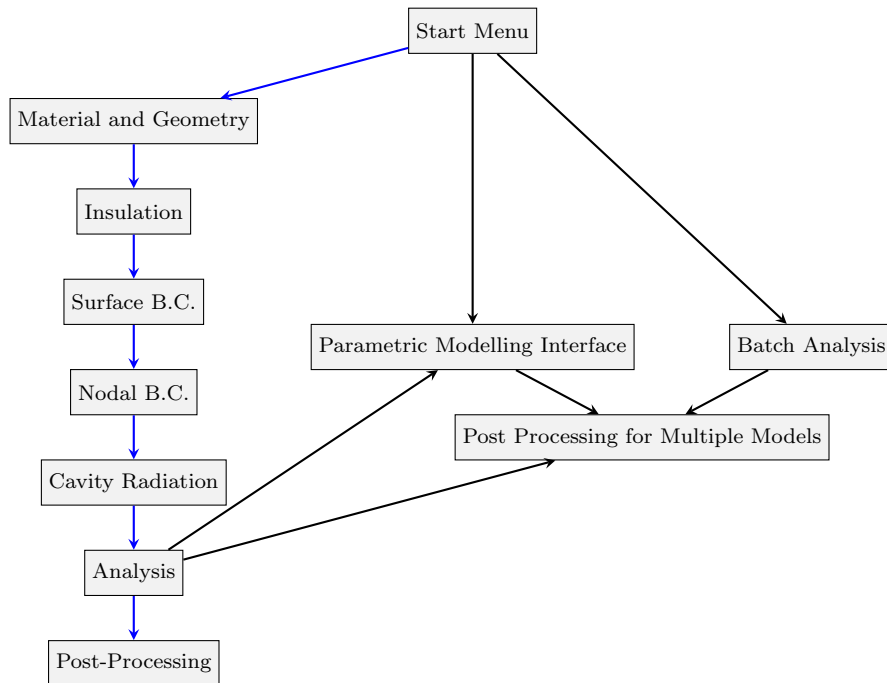


Figure 4.1. Illustration of GUI workflow.

GUI provides three main workflows in modelling to the user. In the first option that is called as Standard GUI Workflow in this document, the user can choose to create a new model and follow the standard GUI workflow as described in Section 4.1, which takes around a few minutes even for an advanced model. In the second option that is called as Batch Analysis in this document, the user can choose to run multiple models (that were created before using the first or third option) at once as described in Section 4.2. As a third option the user can choose to create multiple models in a Parametric Modelling Study as described in Section 4.3.

The user can jump to the results of a previous model that was created using any of the workflows using ‘See Results for a Previously Analyzed Model’ option. Previous batch analyses and parametric studies can also be opened.

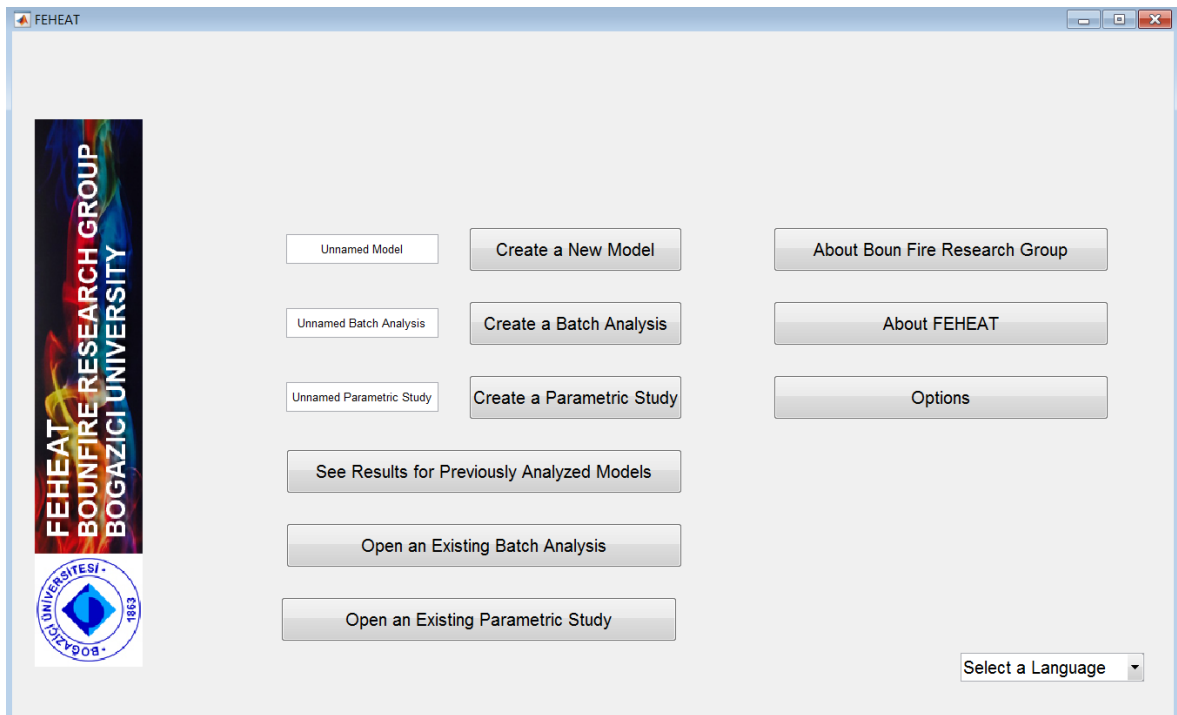


Figure 4.2. ‘Start Screen’ menu.

4.1. Step-by-Step Illustration of ‘Standard GUI Workflow’

4.1.1. ‘Material and Geometry Definition’ Menu

In this menu, material properties, cross-section properties and mesh preferences are taken from the user.

Three options are provided for material properties;

- Choosing available material properties for common materials from the drop-down menu.
- Choosing temperature dependent material properties (see Figure 4.4; user can input conduction coefficient for both directions and specific heat as temperature dependent. Note that density is always taken as constant because (1) it rarely changes dramatically with temperature and (2) time-dependency of density can be taken into account while inputting the specific heat by the user since density is always multiplied with specific heat before entering into any calculation.
- Choosing user-input; user directly specifies constant material properties.

After determination of material properties, the user specifies the cross-section type. Then the user can either choose one of the built-in libraries available for the specified cross-section type or user-defined option to determine the cross-section dimensions. If a library is selected, then the user can select available cross-sections within the specified library. Please note that user can easily create a custom library by modifying `xlsx` files that are available as `Crosssectiontype.xls` (`IShape.xls`, `Box.xls` etc.) in the program directory. User can add a new worksheet in these spreadsheet files, and it will automatically show up in the drop-down menu.

FEHEAT currently supports only quad elements and the user is expected to input the number of divisions across both direction for each parts of the cross-section. This way, mesh generation is easily implemented, and the user has control over it. After

related data are given and ‘Generate’ button is clicked, mesh is generated, and a plot of the meshed cross-section is provided to the user for information. A screenshot during the last step where all information is given for an example project is shown in Figure 4.3. After specifying all the necessary data, the user goes to ‘Insulation Data’ menu by clicking the ‘Next’ button.

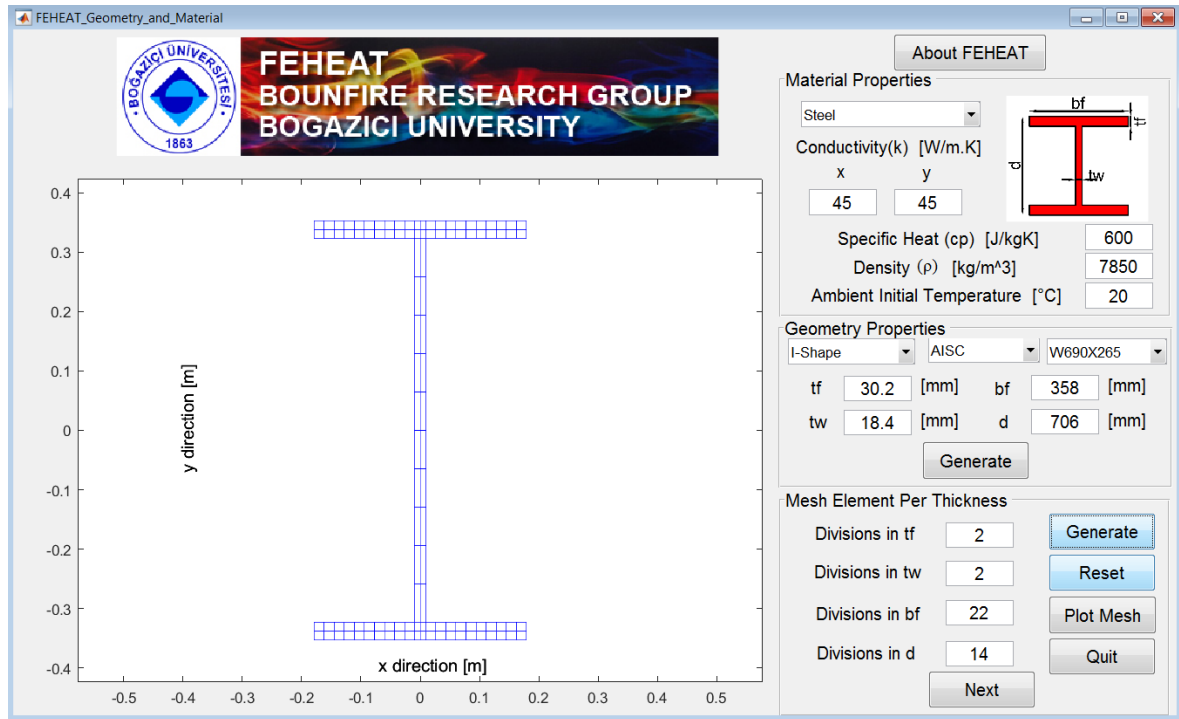


Figure 4.3. ‘Geometry and Material’ menu.

The temperature dependent material properties are filled by the user using the menu shown in Figure 4.4. Material can be saved with a custom name for future use. A two-letter shortcut name is also specified by the user, which is used to refer the material in many menus.

FEHEAT
BOUNFIRE RESEARCH GROUP
BOGAZICI UNIVERSITY

Temperature [C]	kx [W/m.K]	ky [W/m.K]
20	54	54
800	27.3	27.3
1200	27.3	27.3

Temperature [C]	cp [J/kgK]	ρ [kg/m ³]
20	440	7850
100	488	
600	760	
680	890	
720	1388	
735	5000	
750	1483	
770	1002	
900	650	
1200	650	

☒ Save material as:
New Material

Assign a two latter shortcut for quiack menus
NM

Quit

Next

Figure 4.4. 'Temperature Dependent Material Properties' menu.

4.1.2. 'Insulation Data' Menu

In this menu, the user can apply insulation to any of the surfaces using a user-friendly menu. Each surface of the cross-section is assigned a surface number and a sketch of the cross-section with surface numbers is provided to the user. The thickness and the number of divisions across the thickness are inputted for each insulated surface. After specifying the insulation to the surfaces as desired, 'Generate' button regenerates the mesh including insulation elements. The meshed plot of the cross-section is updated with insulation materials added. Insulation elements are coloured different so that they can be distinguished. Clicking the 'Next' button opens 'Insulation Material' menu.

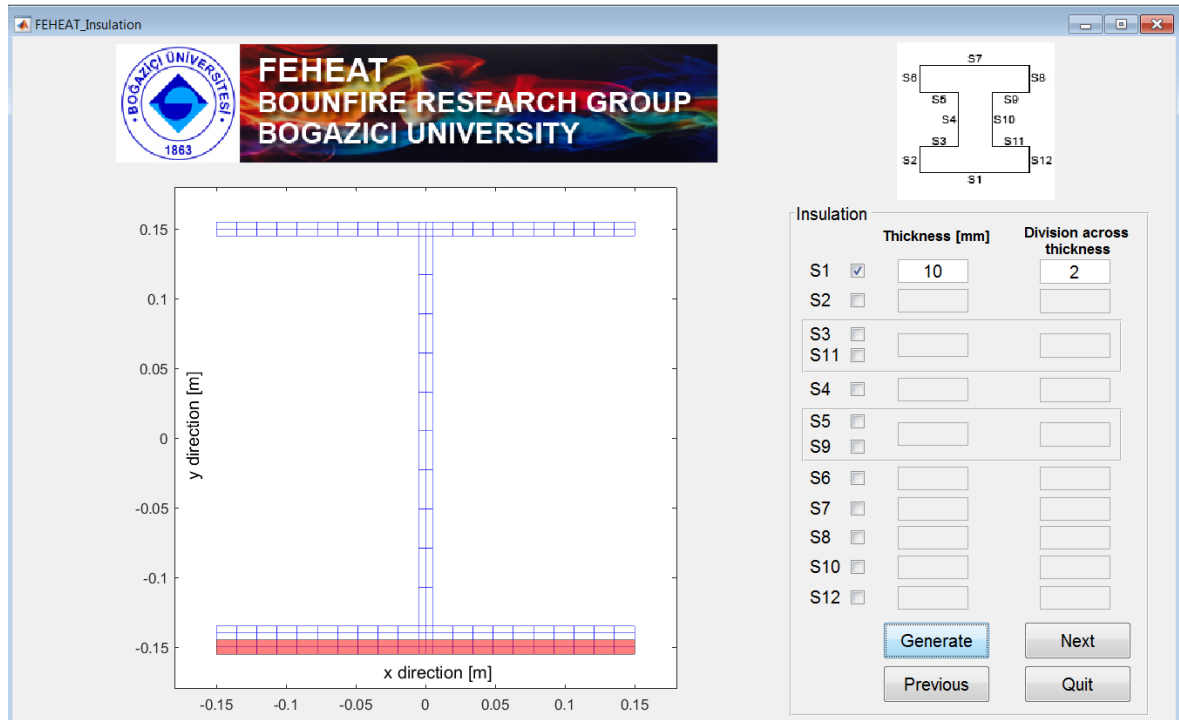


Figure 4.5. ‘Insulation Data’ menu.

In ‘Insulation Material’ menu, material properties are specified for each insulated surface. Like in the material drop-down menu for the cross-section, the user can choose one of the available materials, constant material properties or temperature dependent material properties. Many common insulation materials like Spray Mineral, Fiber Spray, Vermiculit Spray, Perlite Spray, Vermiculit-Cement Spray, Vermiculit-Gypsum Board, Siliceous Fiber Board, Siliceous Cement Board, Gypsum Board and Glass Wool are already available. Specifying the temperature dependent option, will open the same menu that is also used for the cross-section material as shown in Figure 4.4.

4.1.3. ‘Surface Boundary Conditions’ Menu

In this menu the user can define boundary conditions for any of the surfaces on the cross-section. A simple graph of the cross-section with the naming of the surfaces is provided to the user. When the user clicks on a surface on the diagram, the surface is highlighted, and all boundary condition options are activated for that

	Conductivity(k) [W/m.K]		Specific Heat (cp) [J/kgK]	Density (ρ) [kg/m^3]	
	x	y			
S1	0.2	0.2	1700	800	Board Gypsum
S2					Select Material
S3					Select Material
S4					Select Material
S5					Select Material
S6					Select Material
S7					Select Material
S8					Select Material
S9					Select Material
S10					Select Material
S11					Select Material
S12					Select Material

Figure 4.6. 'Insulation Material' menu.

surface. Radiation and/or convection boundary conditions can be defined with constant or varying temperature. Built-in options include ISO834, ISO834 Decay, External, Hydrocarbon, ASTM E119, Constant, User Specified (User specifies temperature-time data manually). The user can save the data given after choosing the user specified to use in future projects.

The user can also specify direct heat flux for selected surface. Surfaces for which direct heat flux is assigned are highlighted in a different colour to distinguish from other boundary conditions. Convection/radiation boundary conditions and direct heat flux boundary conditions cannot be assigned to the same surface. When the user activates one of them for a surface, the other option is deactivated for that surface automatically.

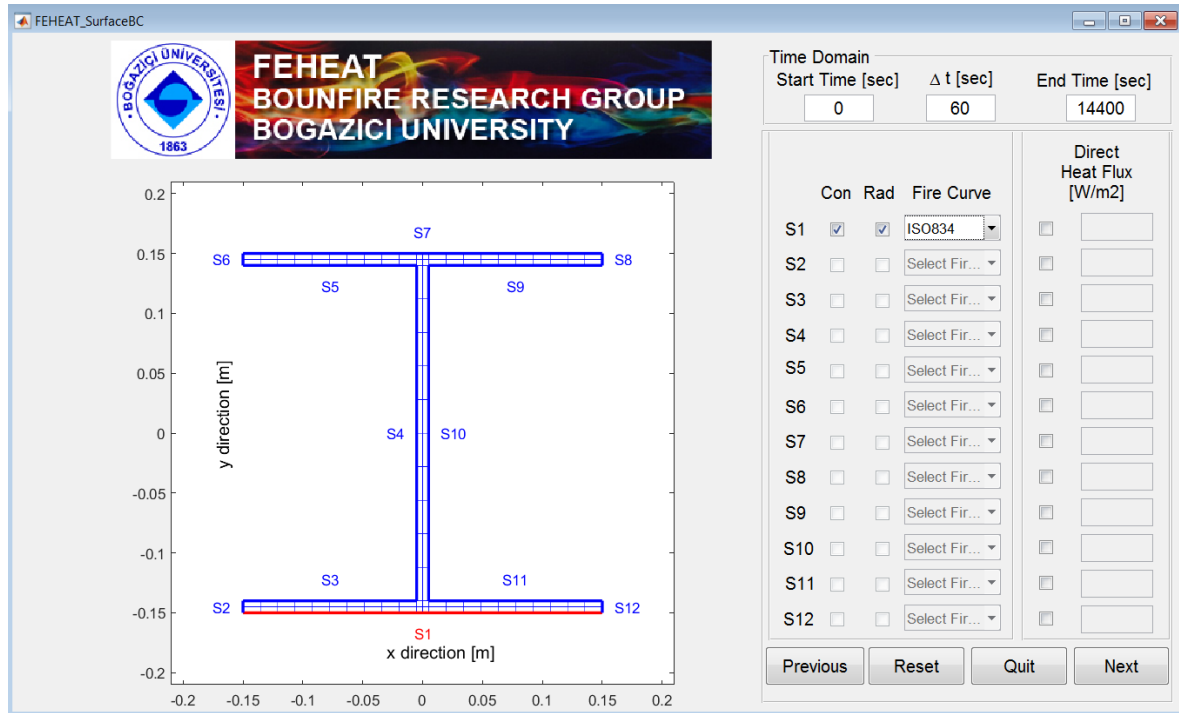


Figure 4.7. 'Surface Boundary Conditions' menu.

4.1.4. 'Prescribed Temperatures and Heat Fluxes for Nodes' Menu

In this menu, the user can specify prescribed temperatures and/or heat fluxes for any of the nodes. A simple graph of the cross-section is given on which the user chooses which nodes to assign values. When the user chooses a node on the diagram, a pop-up menu appears in which the user specifies the prescribed temperature and/or heat flux for that node. Any node for which the user has assigned a value is highlighted on the graph and a list of the nodes and values that were assigned to those nodes are provided to the user. Also, a button is provided to plot the mesh with nodal numbers is added, which can be used to double-check the node numbers.

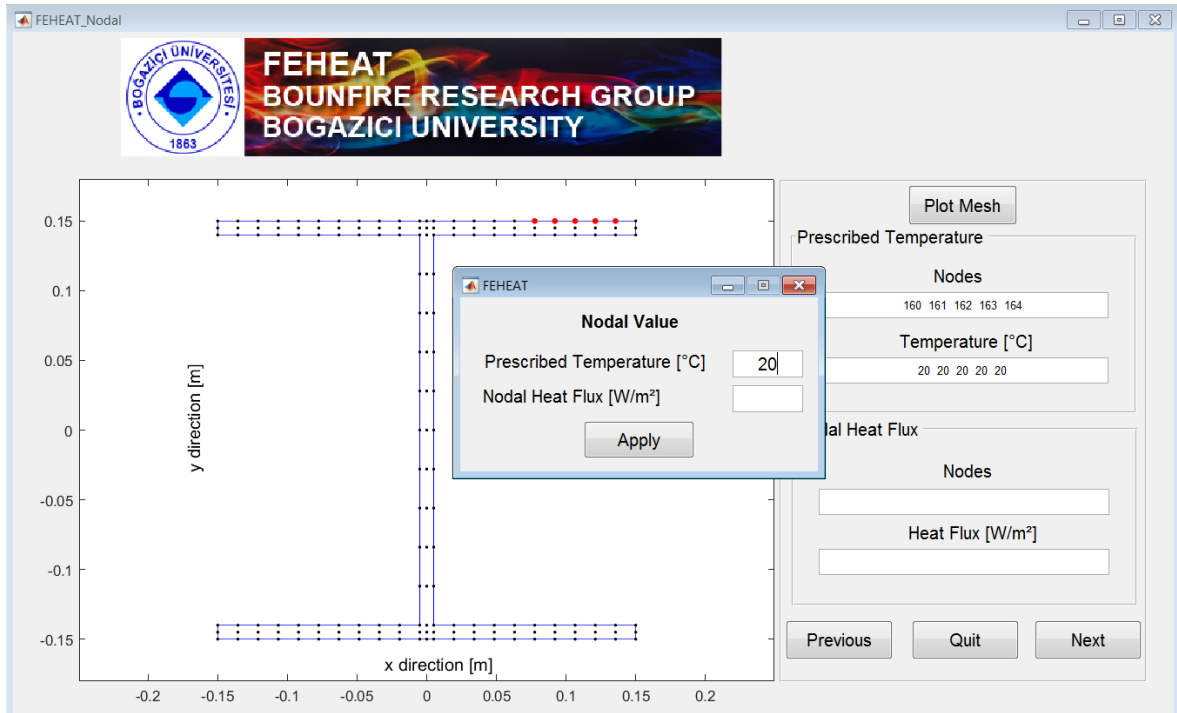


Figure 4.8. ‘Prescribed Temperatures and Heat Fluxes for Nodes’ menu.

4.1.5. ‘Cavity Radiation’ Menu

In this menu, the user specifies if cavity radiation (surface heat exchange) is to be allowed on surfaces. By geometry, there are two cavities for I-Shape and T-Shape, one cavity for Box, Angle, Channel. The user can choose to let one/both (where applicable)/none of them. If rectangular shape is chosen, this menu does not show up since no cavity is available for rectangular shape.

Emissivity is equal to 1 by default for surface heat exchange in cavities and it is not permitted to be changed. Discretization is taken as 6 by default and it is used for view factor calculation as explained in Chapter 2. The user can change both parameters in advanced options provided in start screen.

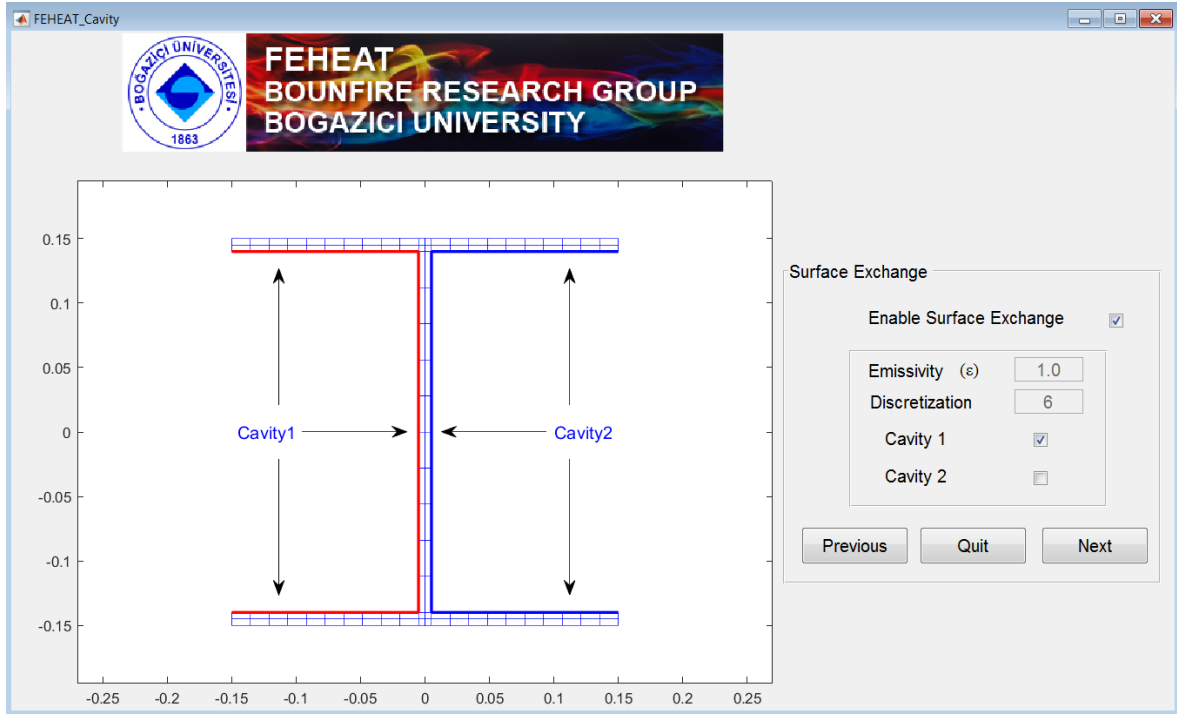


Figure 4.9. ‘Cavity Radiation’ menu.

4.1.6. ‘Analysis and Post-Process’ Menu

This menu is the final step in the standard GUI workflow. The user specifies general analysis parameters like whether to use lumped mass, Newton Raphson Tolerance (TOL). The user also presented a summary of the inputs given so far to the GUI by the user. After specifying general analysis parameters and checking the inputs the user can choose to ‘Write Input Only’ option. Which only creates the input file for analysis and does not start the analysis. Input files created this way can be used in parametric modelling studies as described in Section 4.3 or batch analysis as described in Section 4.2.

‘Run Analysis’ option runs the analysis in the background. The current status on the analysis is shown at the status bar at the bottom left of the window.

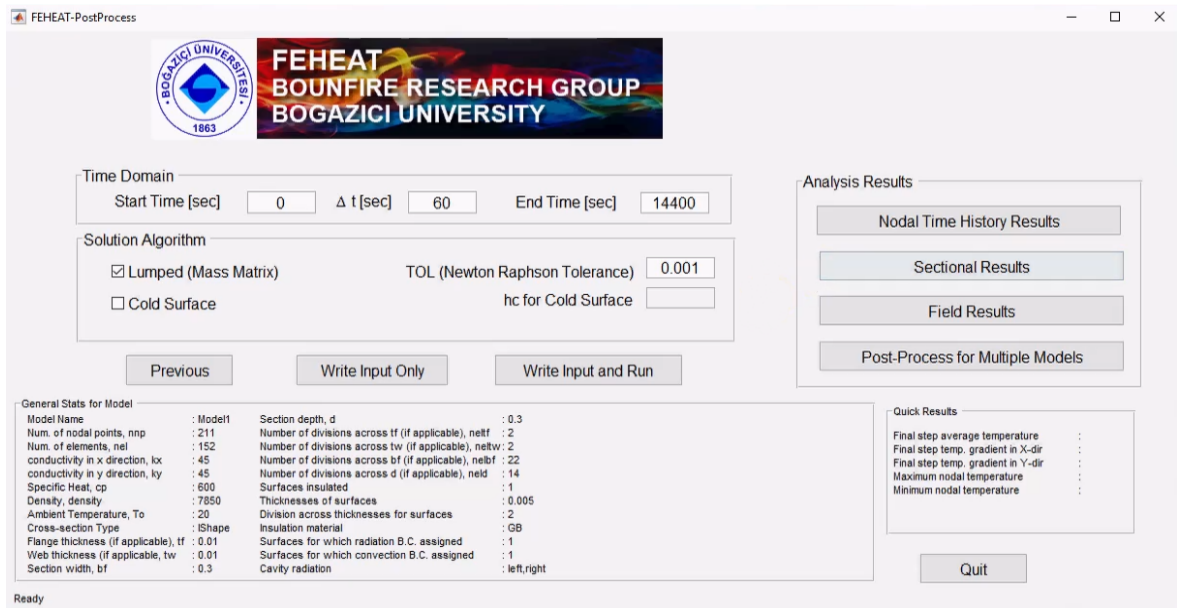


Figure 4.10. ‘Analysis and Post-process’ menu.

After the analysis is complete, three post-processing tools are provided to the user. ‘Nodal Time History Results’ button opens a menu where time history results can be obtained for nodes. ‘Sectional Results’ button opens a menu where average/max/min results can be obtained for a part (top flange, web etc.) of the cross-section. ‘Field Results’ button opens a menu where field results (nodal temperature contour etc.) can be obtained for a specified time step.

Apart from tabulated time history results and contours, some other practical results are also presented. Average temperature on any surface or part (bottom flange, web etc.) of the cross-section for specified time step or as a time-history can be obtained. Average temperature and the thermal gradient for both directions (x and y) can be obtained for the whole cross-section for specified time step or as a time-history.

Thus, the user has the contour graphs to quickly evaluate the results visually. If desired, tabulated results provide extensive ability to evaluate the analysis and can be used to any structural analysis software. Finally, practical results like thermal gradient on the cross-section or average temperature of the cross-section provide meaningful

results for which most of the structural fire engineers are looking for.

4.1.7. ‘Nodal Time History Results’ Menu

In this menu nodal temperatures-time and heat flux-time plots can be obtained. The user first chooses the model file for which the results will be plotted if this menu is called by post-process menu for multiple models. Then the result type is specified by the user. Finally, the node numbers are specified. The user can either specify the node using the node number or can choose the node from a plot of the cross-section that pops up after clicking ‘Pick on Cross-section’ button. Time history results for specified nodes can also be exported to xls or txt files. Single or multiple nodes can be chosen for both plot and export options.

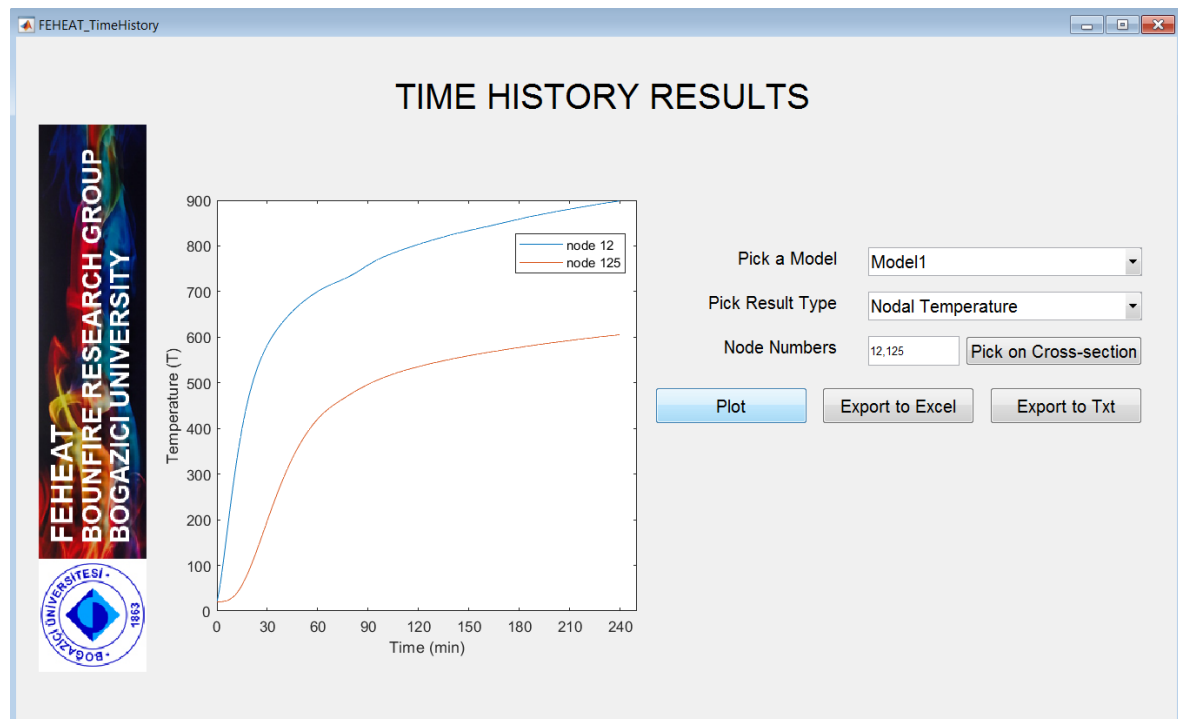


Figure 4.11. ‘Nodal Time History Results’ menu.

4.1.8. ‘Sectional Results’ Menu

In this menu, average/min/max temperature-time plots can be obtained for parts of the cross-section. The user first chooses the model file for which the results will be plotted if this menu is called by post-process menu for multiple models. Then the result type is specified by the user. Finally, the part names (top flange, web, etc.) are specified. The user can choose the part using the drop-down menu from available options. ‘Add to Plot’ button adds the results for the specified part to the plot. Time history results for specified parts can also be exported to xls or txt files. Single or multiple parts can be chosen for both plot and export options.

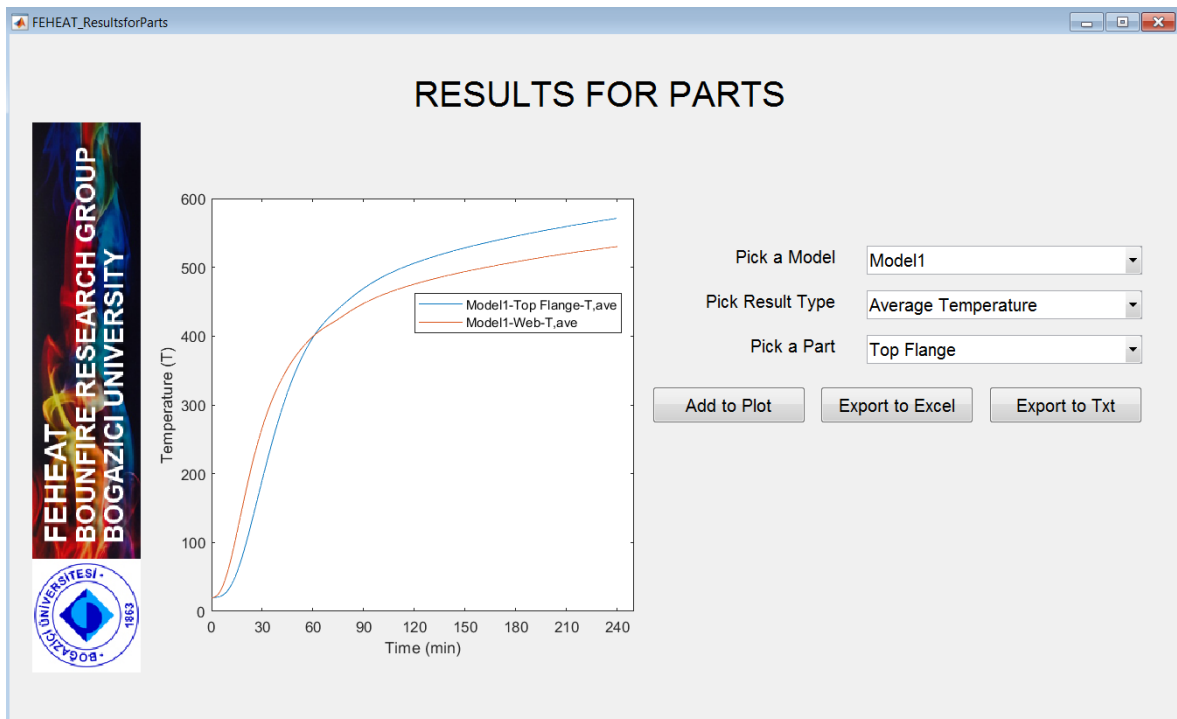


Figure 4.12. ‘Results for Parts’ menu.

4.1.9. 'Field Results' Menu

In this menu, nodal temperature or nodal heat fluxes contour for a specific time step. The user first chooses the model file for which the results will be plotted if this menu is called by post-process menu for multiple models. Then the result type is specified by the user. Either coloured contours or isolines can be plotted. Isolines can only be practical for thick sections since isoline labels cannot be clearly seen in a thin cross-section.

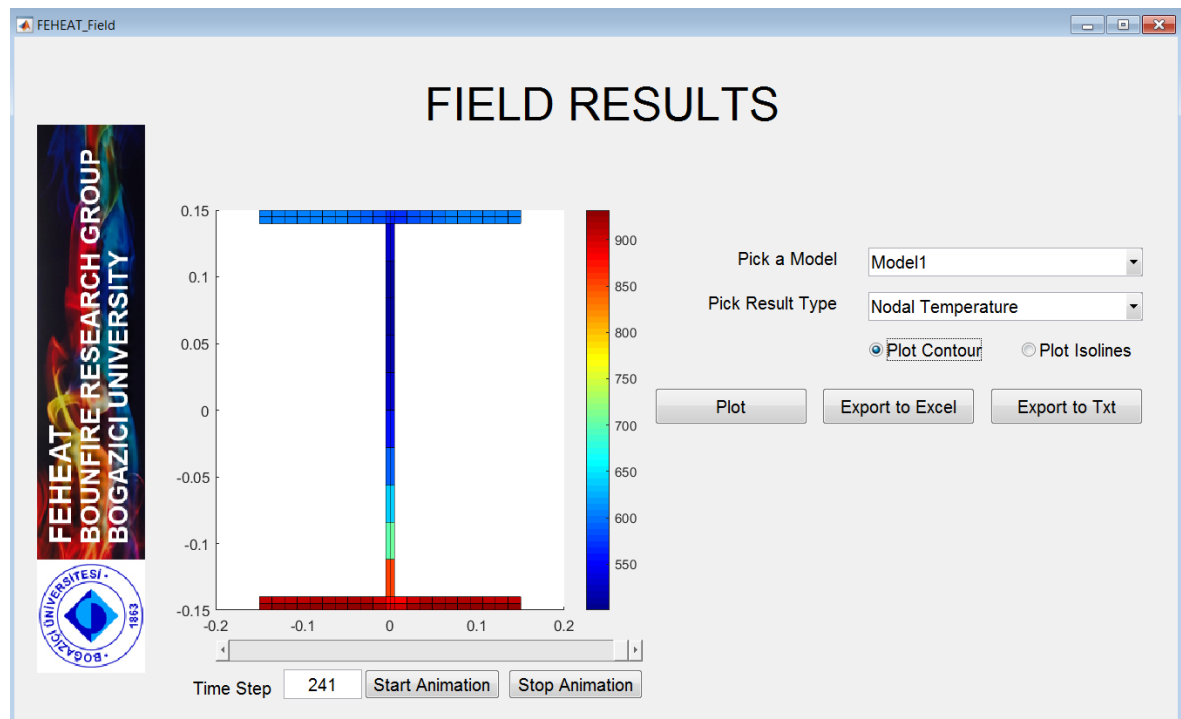


Figure 4.13. 'Field Results' menu.

The plot is first generated for the final step after clicking 'Plot' button. Once the time step is entered by the user, the plot is regenerated automatically. A slider is also added below the graph which simplifies the user input for time step. The plot is regenerated once the slider is moved by the user as well. Additionally, animation through the time history is provided. Once 'Start Animation' button is clicked, the graph animates through the time history.

4.2. 'Batch Analysis' Menu

'Batch Analysis' menu provides the user the ability to run multiple models that were created previously using the standard GUI workflow at once. All analyses are run in the background, and the user is given the information about the analysis status. After all analysis are finished, 'Post-Processing Menu for Multiple Models' (see Figure

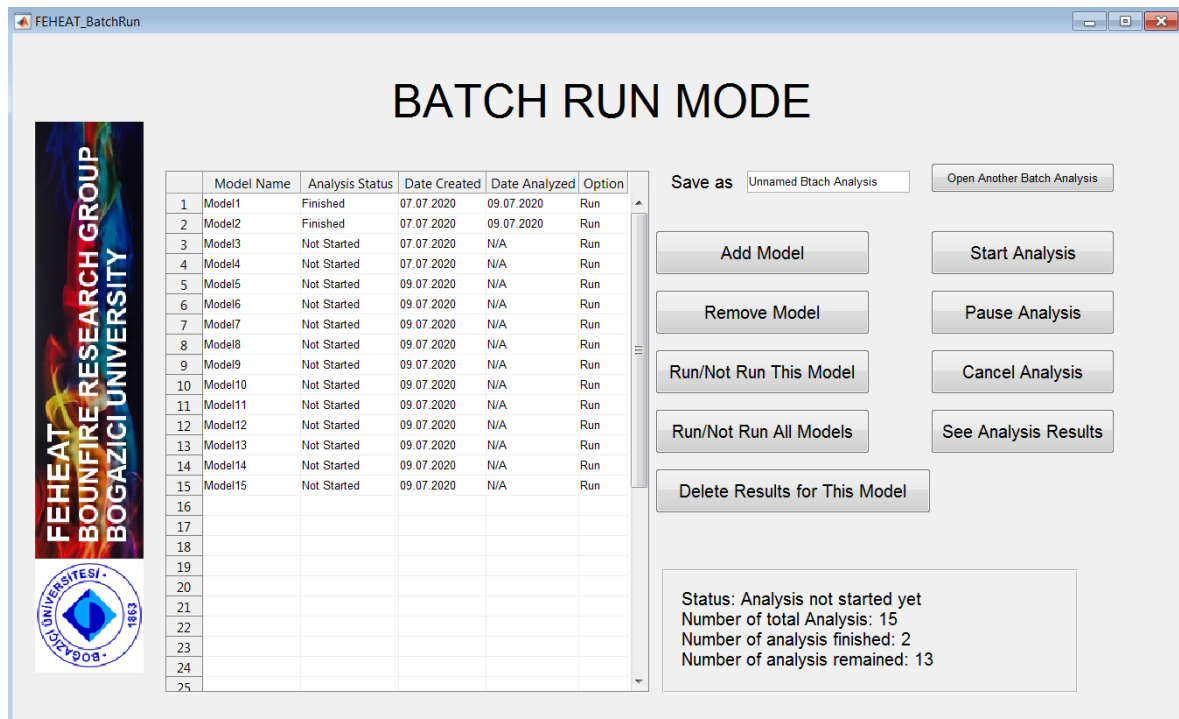


Figure 4.14. 'Batch Analysis' menu.

4.15) is opened. This menu works in a similar way to the one for the standard GUI workflow as described in Section 4.1.6 and Figure 4.10. The difference is that this menu is not for analysis and it is only for post-processing for multiple models.

Available options for post-processing are 'Nodal Time History Results', 'Sectional Results' and 'Field Results'. The menus are described in Sections 4.1.7, 4.1.8, 4.1.9 respectively. This menu provides a powerful tool to compare results for multiple models within the program without the need for an additional tool.

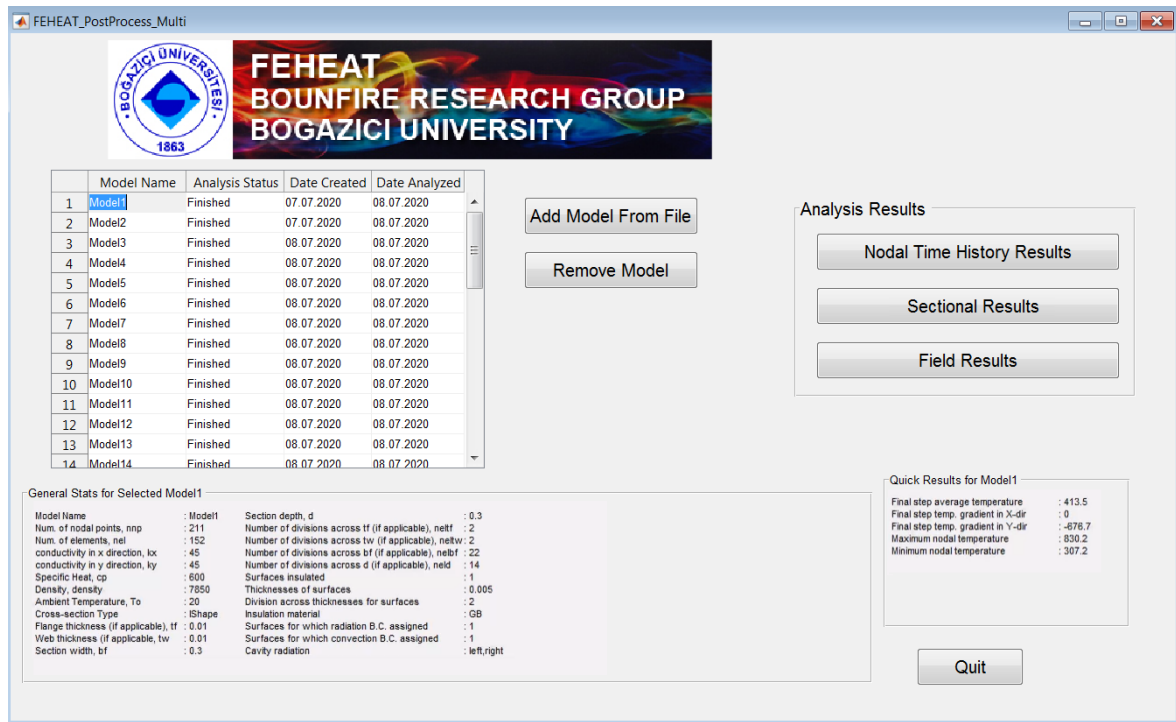


Figure 4.15. ‘Post-Processing Menu for Multiple Models’ menu.

4.3. Parametric Modelling Interface

Parametric Modelling Interface is created to provide the user the ability to make parametric studies without following the standard GUI workflow for each of the models. Providing this interface, FEHEAT becomes a powerful tool for parametric studies in 2D heat transfer analysis.

Once the button ‘Create a Parametric Study’ button is clicked in the start screen, a folder is created in the default directory with the name specified. All models created within the study are stored in this folder. Default directory can be changed to a desired directory in options.

The user can choose a source file from which parameters are to be taken if a parameter is not specified for a model. This way it is not necessary to provide all inputs for models that are very similar to each other with a few exceptions. The source

PARAMERTIC MODELLING INTERFACE

	Model Name	Analysis Status	Source	Date Analyzed	Option
1	Model1	Finished	File 'Model21'	07.07.2020	Run
2	Model2	Not Started	Model1	N/A	Run
3	Model3	Not Started	None	N/A	Run
4	Model4	Not Started	Model1	N/A	Run
5	Model5	Not Started	Model1	N/A	Run
6	Model6	Not Started	Model1	N/A	Run
7	Model7	Not Started	Model1	N/A	Run
8	Model8	Not Started	Model7	N/A	Run
9	Model9	Not Started	Model7	N/A	Run

Buttons: Add Model From File, Add Model, Remove Model, Run/Not Run Selected, Start Analysis, Pause Analysis, Cancel Analysis, See Analysis Results

Parameters for Selected Model

☒ Geometry From Source ☒ Material From Source ☒ Insulation From Source (If Applicable) ☒ Surface Boundary Conditions From Source If Appl...

Geometry: I-Shape, User, Cross-Section Na..., 10 tw, 10 tf, 300 bf, 300 d, 2 div_tw, 2 div_tf, 22 div_bf, 14 div_d

Material: Steel, 45 kx, 45 ky, 650 cp, 7850 density, 20 Ambient

Insulation: Surface Number, Thicknesses, Num of Divisions, Ins Materials

Time Settings: 0 tstart, 60 Dt, 14400 tend

Prescribed Nodal Values: Node Numbers, Prescribed Temperatures, Nodal Heat Fluxes

Surface Boundary Conditions: S1, S2, S3, S4, S5, S6, S7, S8, S9, S10, S11, S12. Options: Con, Rad, FireCurve, Direct Heat Flux.

Analysis Parameters: ☒ Lumped, ☐ Cold Surface, 0.001 TOL, hc-cold

Source Model That Will Be Used for Unspecified Data: From File

Figure 4.16. 'Parametric Modelling Interface' menu example form for source from file option.

model can be from (1) a model previously created using the standard GUI workflow, (2) a model within the current parametric study or (3) none.

If a model is to be created from a source file, the file is called using the button 'Add Model From File'. All parameters are deactivated for models for which source from file option is chosen. But the user can modify the parameters by deactivating 'from source' options if desired. This will not modify the source file and create a new model within the folder specified for the parametric study. In Figure 4.16, Model1 is created using file called Model21 as a source file. In this case no modification is made, and all parameters are used as they are within the source file.

In Figure 4.17, Model2 is created using Model1 as a source model. In this case all parameters are used as they are in Model1 except that insulation with material Gypsum Board (GB) is applied to the bottom of the bottom flange (surface 1). The

thickness is 10 mm and division across the thickness is chosen as 2. In this way two models (one with insulation and the other without insulation) are created with an efficient way.

PARAMERTIC MODELLING INTERFACE

	Model Name	Analysis Status	Source	Date Analyzed	Option
1	Model1	Finished	File 'Model1'	07.07.2020	Run
2	Model2	Not Started	Model1	N/A	Run
3	Model3	Not Started	None	N/A	Run
4	Model4	Not Started	Model1	N/A	Run
5	Model5	Not Started	Model1	N/A	Run
6	Model6	Not Started	Model1	N/A	Run
7	Model7	Not Started	Model1	N/A	Run
8	Model8	Not Started	Model17	N/A	Run
9	Model9	Not Started	Model17	N/A	Run

Buttons: Add Model From File, Add Model, Remove Model, Run/Not Run Selected, Start Analysis, Pause Analysis, Cancel Analysis, See Analysis Results

Parameters for Selected Model

☒ Geometry From Source ☒ Material From Source ☐ Insulation From Source (If Applicable) ☒ Surface Boundary Conditions From Source If Applicable

Cross-Section Type: Steel
Library: [Dropdown]
Cross-Section Name: [Dropdown]

Material Properties: kx, ky, cp, density, Ambient

Insulation: 1 (Surface Number), 10 (Thicknesses), 2 (Num of Divisions), GB (Ins Materials)

Time Settings: tstart, Dt, tend

Prescribed Nodal Values: Node Numbers, Prescribed Temperatures, Nodal Heat Fluxes

Surface Boundary Conditions: S1-S6, S7-S12 (Con, Rad, FireCurve, Direct Heat Flux)

Analysis Parameters: Lumped, Cold Surface, TOL, hc-cold


Source Model That Will Be Used for Unspecified Data: Model1

Figure 4.17. 'Parametric Modelling Interface' menu example form for source from model option.

As a final option the user can create a model from scratch using the parametric modelling interface. In this case the source model is chose as 'None' and all parameters are specified by the user for the model. In Figure 4.18, Model3 is created from scratch and all parameters are specified for the model.

FEHEAT_ParametricStudy

PARAMERTIC MODELLING INTERFACE



	Model Name	Analysis Status	Source	Date Analyzed	Option
1	Model1	Finished	File 'Model1'	07.07.2020	Run
2	Model2	Not Started	Model1	N/A	Run
3	Model3	Not Started	None	N/A	Run
4	Model4	Not Started	Model1	N/A	Run
5	Model5	Not Started	Model1	N/A	Run
6	Model6	Not Started	Model1	N/A	Run
7	Model7	Not Started	Model1	N/A	Run
8	Model8	Not Started	Model7	N/A	Run
9	Model9	Not Started	Model7	N/A	Run

Add Model From File

Add Model

Remove Model

Run/Not Run Selected

Start Analysis

Pause Analysis

Cancel Analysis

See Analysis Results

Parameters for Selected Model

☐ Geometry From Source

I-Shape: User

Cross-Section Na...: 20 tw 2 div_tw 300 bf 22 div_bf 435 d 22 div_d

☐ Time From Source

Time Settings: 0 tstart 60 Dt 14400 tend

☐ Material From Source

Steel: 45 kx 45 ky 650 cp 7850 density 20 Ambient

☐ Prescribed Nodal Values From Source

Prescribed Nodal Values: Node Numbers Prescribed Temperatures Nodal Heat Fluxes

☐ Insulation From Source (If Applicable)

Insulation: Surface Number Thicknesses Num of Divisions Ins Materials

☐ Surface Boundary Conditions From Source If Appli...

Surface Boundary Conditions:

Surface	Con	Rad	ISO	FireCurve	Direct Heat Flux
S1	<input checked="" type="checkbox"/>	<input checked="" type="checkbox"/>	ISO		
S2	<input checked="" type="checkbox"/>	<input checked="" type="checkbox"/>	ISO		
S3	<input type="checkbox"/>	<input type="checkbox"/>	FireCurve		
S4	<input type="checkbox"/>	<input type="checkbox"/>	FireCurve		
S5	<input type="checkbox"/>	<input type="checkbox"/>	FireCurve		
S6	<input type="checkbox"/>	<input type="checkbox"/>	FireCurve		
S7	<input type="checkbox"/>	<input type="checkbox"/>	FireCurve		
S8	<input type="checkbox"/>	<input type="checkbox"/>	FireCurve		
S9	<input type="checkbox"/>	<input type="checkbox"/>	FireCurve		
S10	<input type="checkbox"/>	<input type="checkbox"/>	FireCurve		
S11	<input type="checkbox"/>	<input type="checkbox"/>	FireCurve		
S12	<input checked="" type="checkbox"/>	<input checked="" type="checkbox"/>	ISO		

☐ Cavity From Source If Applicable

Surface Exchange Options: ☐ Enable Surface Heat Exchange ☐ Cavity1 ☐ Cavity2

☐ Analysis Parameters From Source

Analysis Parameters: ☐ Lumped ☐ Cold Surface 0.001 TOL hc-cold

Source Model That Will Be Used for Unspecified Data: None

See Units

Figure 4.18. 'Parametric Modelling Interface' menu example form for source from none option.

5. CONCLUSION

5.1. Summary

With increased use of the performance-based approach, the proper design of the fire protection strategy and structural detailing of a building is more based on evaluating the structure's behaviour under realistic fire scenarios. Thus, the accurate determination of temperature distribution on a cross-section under fire is gaining more importance on structural fire engineering practice. FEHEAT has been developed by Serdar Selamet [5] to provide a tool that helps structural fire engineers achieve this. With this study, FEHEAT is further developed and also gained a graphical user interface (GUI).

As an outcome of this study FEHEAT gains the ability to consider temperature dependent material data. The nonlinear solution algorithm is developed to consider nonlinearities in material properties by modifying the tangent stiffness matrix. The code handles most nonlinearities in material properties with a few additional iterations and is proven to handle very sudden peaks (like the specific heat of steel) with additional iterations, as necessary.

Finite element formulation was developed considering all possible boundary conditions including radiation due to fire, radiation due to surface heat exchange, convection, Dirichlet and Neumann boundary conditions. A semi-discrete time stepping algorithm was developed in for time history analysis. Nonlinear solution algorithm which is activated only when radiation boundary conditions and/or nonlinear material properties exist provides an efficient tool for nonlinear analysis.

Validations for different scenarios were made by comparing FEHEAT with ABAQUS. Verifications include radiation, surface heat exchange, convection, insulation considering different cross-section types. It is shown that FEHEAT can handle any of the

problems that are faced in classic two-dimensional heat transfer analysis with great accuracy. All modelling was made using the GUI designed within the scope of this study.

Within this study, graphical user interface was designed such that it provides a user-friendly experience to the user while modelling with provided features like built-in libraries (for cross-sections, materials, insulations, fire curves, etc.), graphical illustration of the user inputs (mesh of the cross-section, coloring boundaries where a boundary condition is assigned, highlighting the nodes for which a prescribed temperature or nodal heat flux is assigned, etc.), extensive post-processing tools (time history plots and tables, temperature contours, etc.).

GUI also provides batch analysis tool which is used for analysis of multiple models at once. This is helpful when too many and/or too heavy models are to be run at once and compared or multi-processed. Post-processing menu for multiple models is also provided to help compare results of multiple models.

Another tool that is provided by GUI is the parametric modelling interface, which can be used to perform an extensive parametric study considering any parameter of the general heat transfer problem as a variable. It is aimed with this tool that, FEHEAT will be a powerful software that is used for parametric studies in two-dimensional heat transfer analyses as well apart from being used in practise by the structural engineers (which was the original motive of the development of FEHEAT).

FEHEAT is designed for heat transfer analysis but outputs are what a structural engineer needs in structural analysis or performance evaluation of the cross-section under fire.

Another motivation to this study was the need for a domestic software in structural engineering field with a focus on heat transfer as there is none in this area. FEHEAT is also the first software produced within the civil engineering department of

Boğaziçi University. As the software development by civil engineers is rarely seen, it is hoped that this study and previous studies for the development of FEHEAT will be an inspiration for the future studies in this area.

5.2. Possible Improvements

Although FEHEAT was designed as a heat transfer analysis software, it is possible that this study can be further developed such that a hybrid analysis software that can handle both heat transfer and structural analysis. Currently, FEHEAT provides all the necessary data that can be obtained from a heat transfer analysis and can be used for a structural analysis but does not have a previous study on evolving into a software that can perform structural analysis.

The code is limited to 2D analysis but can easily be extended to be able to solve three-dimensional problems. The main code that performs the analysis mostly compatible to a three-dimensional analysis. But such an improvement requires an extensive study in graphical user interface (GUI). Additionally, three-dimensional heat transfer analyses are not widely used in structural engineering field as most of the problems faced can be solved with a two-dimensional analysis.

FEHEAT currently supports cross-section classes of I-Shape, Box, Angle, Channel, T-Shape and solid rectangle only. Additional cross-section classes like solid circular, circular hollow (CHS) can be (and planned to be) added in future releases. Such implementation will require triangular finite elements to be employed. Direct import of the cross-section of any shape from a dxf file is also planned to be added in future releases with the development of a general meshing tool for implementing triangular and quad elements together.

FEHEAT provides outputs in the form of graph and tabulated data. Tabulated data can be imported to any software for further studies (like structural analysis). Automation of this process could be a helpful and integration with common structural

analysis software can be made for future releases. This is typically obtained designing add-ins inside the target software.

5.3. Areas of Use

FEHEAT was created for the use of structural engineers in their daily projects. For this purpose, the software interface was designed as practical as possible. It can handle any of the common problems in heat transfer analysis that a structural fire engineer face.

FEHEAT provides necessary data for a structural analysis of a structural member. Using temperature distributions provided for each mesh on the cross-section, one can identify the change of mechanical properties for each mesh.

Increase of temperature results in an elongation demand on the structural member. When restraint, this demand results in thermally-induced stresses. Which should also be taken into account in a structural analysis of fire exposed structures.

FEHEAT also provides quick results like average temperature, temperature gradient in both directions. These quick results help the user to make a quick decision on the analysis results. For some cases these results are enough to make a decision depending on the complexity of the problem.

Additionally, FEHEAT does not limit the modelling power to the provided default settings or common problems. The user can also use the software for very advanced analysis by specifying custom data for related properties.

Finally, FEHEAT can be used for parametric studies of structural engineers and academics. The software provides the ability to conduct an extensive parametric study. Modelling phase is extremely simplified by the use of the source models, which is crucial to conduct a complex parametric study.

REFERENCES

1. Hall, J. R., *High-Rise Building Fires*, National Fire Protection Association, Quincy, MA, USA, 2016.
2. *ABAQUS[Computer Software]*, Dassault Systèmes, Providence, RI, USA.
3. *TASEFplus[Computer Software]*, Ulf Wickström and Kuldeep Viridi.
4. *SAFIR[Computer Software]*, the University of Liege.
5. Selamet, S., *Behavior, Design and Finite Element Modeling of Shear Connections Under Fire Hazard.*, Ph.D. Thesis, Princeton University, Princeton, NJ, 2011.
6. Selamet, S., “Thermal Gradient Estimation due to Surface Heat Exchange in Steel I-Sections”, *Journal of Structural Engineering*, Vol. 143, No. 9, pp. 1–1, 2017.
7. *MATLAB[Computer Software]*, MathWorks, Natick, MA, USA.
8. CEN (European Committee for Standardization), “*Design of Concrete Structures.1-2: General Rules - Structural Fire Design*”, *Eurocode 2, EN 1992-1-2*, Brussels, Belgium, 2004.
9. Fu, H. C., S. F. Ng and M. S. Cheung, “Thermal Behavior of Composite Bridges”, *Journal of Structural Engineering*, Vol. 116, No. 12, pp. 3302–3323, 1990.
10. Tan, K.-H. and Z.-F. Huang, “Structural Responses of Axially Restrained Steel Beams with Semirigid Moment Connection in Fire”, *Journal of Structural Engineering*, Vol. 131, No. 4, pp. 541–551, 2005.
11. Selamet, S. and M. E. Garlock, “Plate Buckling Strength of Steel Wide-Flange Sections at Elevated Temperatures”, *Journal of Structural Engineering*, Vol. 68,

- No. 11, pp. 1853–1865, 2013.
12. Selamet, S. and M. E. Garlock, “Fire Resistance of Steel Shear Connections”, *Fire Safety Journal*, Vol. 139, pp. 52–60, 2014.
 13. Shapiro, A. B., “Computer Implementation, Accuracy, and Timing of Radiation View Factor Algorithms”, *Journal Heat Transfer*, Vol. 107, No. 2, pp. 730–732, 1985.
 14. Emery, A. F., O. Johansson, M. Lobo and A. Abrous, “A Comparative Study of Methods for Computing the Diffuse Radiation Viewfactors for Complex Structures”, *Journal Heat Transfer*, Vol. 113, No. 2, pp. 413–422, 1991.
 15. Huebner, K., D. L. Dewhirst, D. E. Smith and T. G. Byrom, *The Finite Element Method for Engineers*, Wiley, New York, USA, 2nd edn., 2008.
 16. Hughes, T. J. R., *The Finite Element Method: Linear Static and Dynamic Finite Element Analysis*, Dover Publications, Mineola, New York, USA, 2000.
 17. *Abaqus 6.11 Theory Manual*, Dassault Systèmes, Providence, RI, USA, 2011.
 18. Bergheau, J. M. and R. Fortunier, *Finite Element Simulation of Heat Transfer*, John Wiley Sons, Hoboken, NJ, USA, 2008.
 19. CEN (European Committee for Standardization), “*Design of Steel Structures.1-2: General Rules - Structural Fire Design*”, *Eurocode 3, EN 1993-1-2*, Brussels, Belgium, 2004.
 20. CEN (European Committee for Standardization), “*Actions on Structures.1-2: General Actions - Actions on Structures Exposed to Fire*”, *Eurocode 1, EN 1991-1-2*, Brussels, Belgium, 2002.